Percolation phenomenon of ceramic metal composites for energy storage applications

Submitted by

Aaqib Mehmood Malik

School of Chemical and Material Engineering

National University of Sciences and Technology

2022

Percolation phenomenon of ceramic metal composites for energy storage applications

Name: AAQIB MEHMOOD MALIK

Reg. No: 00000277426

This thesis is submitted as partial fulfillment of the Requirements

for the degree of

MS in Nanoscience and Engineering

Supervisor Name: Dr. Mohsin saleem

School of Chemical and Materials Engineering (SCME)

National University of Sciences and Technology (NUST)

H-12 Islamabad, Pakistan

August,2022

Dedications

This study is sincerely dedicated to my beloved family, who have been my source of inspiration and gave me strength when I thought of giving up, who continually provide their moral, spiritual, emotional, and financial Support.

Acknowledgments

Abstract

In the present study solid state reaction method is used for the synthesis of copper barium titanate (BaTiO$_3$-Cu) composites in an inert atmosphere. Cu particles were successfully mixed with barium titanate and the resultant Cu-BaTiO$_3$ composites with different concentrations ranging from (5-20% vol) showed high dielectric performance according to percolation phenomenon it is further seen that with the enhancement of copper content in a barium titanate powder the permittivity was significantly increased in the results shown by different techniques. Following Dielectric tests are performed for the dielectric analysis of prepared samples. Dielectric test with different temperatures and frequencies ranging from I0^2 Hz to 1 KHz, real and imaginary part of impedance, relative density and breakdown strength were performed. For the structural and surface morphology analysis the XRD, SEM, RAMAN and FTIR were performed, no major impurities and side reaction took place during calcination and sintering process. SEM images exhibiting uniform and homogenous grain growth of particles in sintering and resulting the formation of grains with a relatively smaller size. This work concluded that Cu-BaTiO$_3$ is an excellent material for high dielectric constants.

Contents

Table of figures

LIST OF ABBREVIATIONS:

PZT	Lead Zirconate Titanate
PLZT	Lead lanthanum zirconate titanate
TGA	Thermogravimetric analysis
SEM	Scanning electron microscopy
XRD	X-ray diffraction
FTIR	Fourier transform infrared spectroscopy
Ba	Barium
ε_r	Dielectric permittivity
T_c	Curie temperature
Re(Z)	Real part of impedance
$Z^{/}$	Real part of impedance
$Z^{//}$	Imaginary part of impedance
P_r	Polarization retention
P_s	Polarization saturation
FE	Ferroelectric
DEC	Dielectric Constant

Chapter No 1
INTORDUCTION

1.1 Introduction:

In the world, electrical storage is rising as a new central issue for microelectronic devices and capacitive devices. This is leading to high demand for electrical devices as a good absorbance and as a good electrical supplier. In other words, we need a material that can bear and accumulate high electrical energy for storage devices. Dielectric materials are used at a large scale in all industries, including commercial and military applications. Due to their processability and low-cost production dielectric materials are usually used for many applications. Depending upon the polarizability of dielectric materials usually, barium titanate and lead zirconate titanate have very high dielectric constants researchers are still working on the development of capacitors for obtaining high dielectric constants by producing many other ceramic-metal composites and capacitors to investigate the dielectric properties and energy storage applications

1.2 Percolation Theory

In the past dielectric are very promising materials for high-energy storage in electronics and motivations are leading toward the miniaturization of the electronic device. For the fabrication of capacitive components with high permittivity (high k) high permittivity results in high energy density and smaller sizes of electronic components. As it is well known that the physical properties of materials are dramatically changes near their percolation threshold point researchers have paid much attention to the percolation composites and suggested them as very promising materials.

To tune the properties of a dielectric material, like to enhance the dielectric constant, low loss, high permittivity, and electrical tune ability many modifications were made to the materials. Some materials are modified with the addition of metals in dielectric materials known as metal fillers in a matrix. To obtain dielectric materials polymer composites materials are also the area of research for many scientists by the addition of metals in composites materials high weight is emerging as a new problem. After all discussion, it is found that low loss and the low threshold are still

a challenge for researchers as well as scientists. A porous ceramic-metal composite is a good technique to get all desired properties a very small amount is required to make the conductive path inside the materials by using conductive metals like copper, silver, and many others.

The main objective of this research is to enhance the dielectric constant materials with high permittivity low loss and low threshold. A solid-state chemical route is adopted for the synthesis of barium titanate. After the synthesis of barium titanate copper nanoparticles is added to the barium titanate powder with different concentrations ranging from (0 to 20% vol) in powder. For surface morphology and structural analysis, the XRD and SEM are performed. Dielectric constant with temperature and different frequencies and impedance analysis is performed under the LCR meter.

Dielectric materials are emerging as a new source of hope in the world which made the electronic component fast and efficient. The performance of dielectric materials has been gradually improving year by year in the last few years very rapidly The widespread use of dielectric materials in electronic components made the world very innovative.
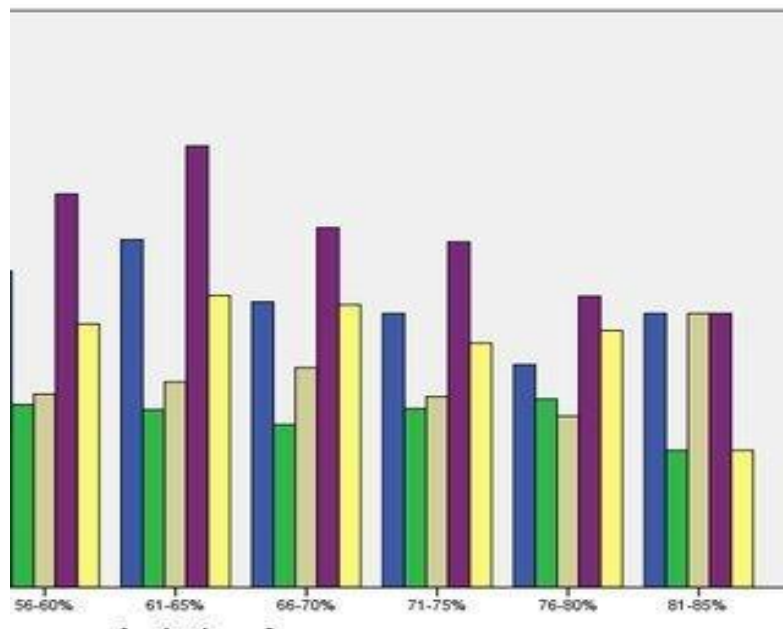
Figure 0-1 Schematic of dielectric performance

1.3 Composites materials

Composite materials are made up of two or more constituents in a matrix. To change the physical and chemical properties of materials, composite materials are the most emerging term. We can tune the electrical, biological, chemical, and mechanical properties of the materials. The composite material consists of two main parts one is a matrix and the other one is reinforcement.

Matrix: Matrix is the continuous and regular geometrical structure or template in which composite is embedded. It can be a metal, polymer, or ceramic material. The matrix provides the medium which gives adhesion, holding and embedded the material or reinforcement into a solid form.

Reinforcement: It provides reinforcement and rigidity. There are three main types of matrices.

- Metal matrix composite materials
- Ceramic matrix composites materials.
- Organic, polymer matrix composites materials.
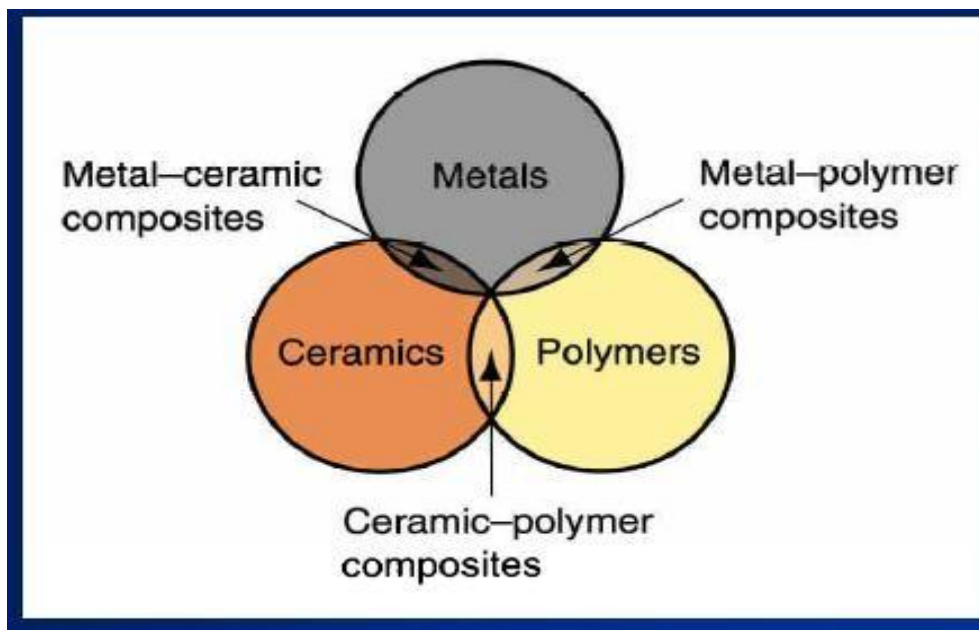
Figure 0-2 Composites materials and their types

1.4 X-rays Diffraction

XRD is a very good approach to studying the chemical formation for elemental analysis as well as phase analysis. It provides information about structures phases, preferred crystal orientation, and the other structural parameters which are given as follows

- Grain size by Debye Scherer formula.
- Crystallinity
- Strain
- Crystal defects

When a beam of a single wavelength of light is irradiated on the sample or powder the x-rays produced are scattered by the lattices planes in the powder after the scattering these waves superpose with each other resulting in the constructive and destructive interference at specifics angles by each set of lattices planes present in crystals planes. Atoms present on the lattice points scattered these rays at different angles the peaks are the image of these lattice atoms. For every specific plane, the arrangement has itsspecific peak at a specific angle in the XRD structure, which confirms the structure of the materials. [1,2]

The working principle of x rays diffraction is when monochromatic light is fall on the interatomic planes it gets scattered at some angles these diffracted rays exhibit constructive and destructive interferences [3].
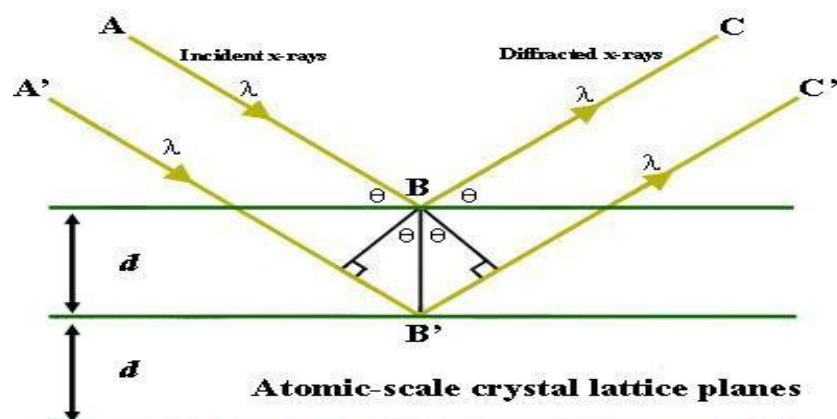
Figure 0-3 X rays diffraction and brags law

Figure 1-2 X rays diffraction and brags law

Where

λ = wavelength of incident light Ө = angle of incidence

d = Inter planar distance

n = order of diffraction

Diffraction depends on the type of unit cell when the X-ray beam is irradiated over the material these rays interact with atomic planes in crystalline or polycrystalline material, they are scattered in specific directions called X-rays scattering a diffractometer received these rays and measures the peaks. An instrument to measure x-ray diffraction is called a diffractometer. Interatomic planes scatter these rays. They exhibit constructive and destructive interference. By changing the direction of detectors all diffracted rays can be detected.

Diffractometer consist of a radiation source, a slit, and a monochromator. Firstly, light passes through the monochromator which filters the light into a single wavelength. A single wavelength of light falls on the sample and scattered the diffracted rays. For polycrystalline the rays diffracted in all possible directions. Detector capture all rays depending upon the orientation of atoms within crystals.

Many facts and Figures pick up by using XRD based on dual nature particle and wave nature. In XRD, a beam of X-ray contains wavelength falls on the powder sample, this beam is reflected from the plan of crystal. The interference only takes place when the incident angle is precisely the same as the reflection angle. Bragg's Law illustrates the diffraction of X-rays by crystals.

$$n \, \lambda = 2d \, Sin\theta$$

λ is X-ray wavelength.

d is a separation between microscopy planes. λ is X-ray wavelength.
$Sin\theta$ is the angle between the incident beam and reflected
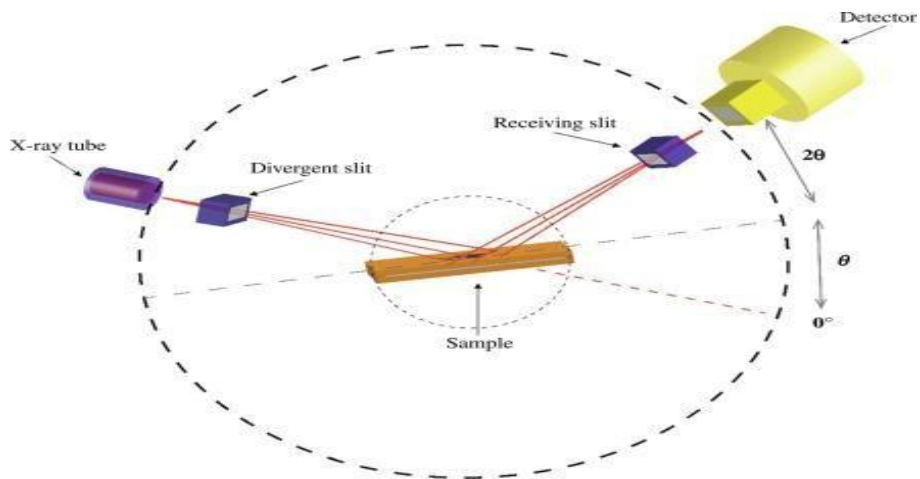
Figure 0-4 Working principle of XRD

The Braggs law stated that the incident ray is only reflected when the path difference between planes is 2d Sin θ. The glancing angle and the wavelength is having an inverse relation to each other. The greater the angle smaller the wavelength, and vice versa. [34]. The condition mentioned above that reflection only occurs when θ ≥ 2d. The working principle and schematic are shown in the above figure

The procedure of this experiment includes the crushing of samples into fine powder. Afterward, the model will be placed on an aluminum or glass rectangular-shaped plate. A monochromatic X-ray beam is then directed towards the powder sample.

1.4.1 Lattice Constant:

Crystal unit cell called lattice constant. Angle forming between two edges or the length of one edge. It is also called the lattice parameter. The lattice constant is the distance between the lattice points; the following equation calculates the lattice constant.

$$\alpha = \frac{\lambda (h2 + k2 + l2)1/2}{2 sin\theta}$$

The above equation shows that the lattice constant is (α) the wavelength of X-ray incident is 1.54Å for Cuk (α), miller indices

1.4.2 Crystallite Size:

For the identification and confirmation of the experimentally obtained diffraction pattern, it is compared to JCPDS cards. The structural properties are greatly influenced by particle size. The XRD perfectly measures the homogeneous and inhomogeneous peaks of the nanomaterial. Strains in the inhomogeneous material vary from crystal to crystal within a single crystal and by increasing angle the broad range of diffraction peaks. Scherer's formula can be used for the calculation of crystallite size D can be estimated from peak width [35]

$$\mathbf{D} = \frac{K\lambda}{B\ Cos\theta}$$

B in the above equation denotes full width half maximum. θ is the angle called

diffraction angle.

K is known as Scherer's constant depending upon crystal size.

1.4.3 X-Ray density

Using XRD, material density can be found, and by applying the formula, we can calculate the material density if lattice constant α know for each sample.

$$\rho_x = \frac{8M}{Na3}$$

1.4.4 Measured Density:

The measured density tells us about the intrinsic properties of materials that define bulk density or measured density. The formula generally used for calculation

$$\rho_m = \frac{m}{\pi\ r2h}$$

'm' represents mass, 'r' represents the radius, and 'h' represents the thickness of the pressed pallet.

1.4.5 Porosity Density:

Porosity density shows the pellet's strength and the state or property of being porous. By increasing the concentration of doping material in the sample, the porosity fraction increased. By using the formula

$$\textbf{Porosity fraction} = \textbf{1-} \frac{\overline{\rho \textbf{m}}}{\rho \textbf{x}}$$

$$\rho$$

1.5   Fourier transform spectroscopy (FTIR)

Both determination and verification of the structure of a compound can be carried out by using IR spectroscopy usually a range from 400 cm to 4000 cm is applied to the sample for this technique known as IR spectroscopy. This is a qualitative study in which the IR spectrum interacts with the vibrational bonds.

Atom and molecules are interconnected by bonds ionic bonds, covalent bonds, and triple covalent bonds. These bonds are always in constant vibrational modes. When the IR spectrum is irradiated over the sample the frequency of vibrational bonds and IR spectrum matches the absorption of electromagnetic radiation takes place and a peak is generated in the graph[7,8]. Thus every peak in the IR spectroscopy is absorption of some specific bonds present in the sample. The Infrared radiations are emitted out from a shining black-body source. An aperture can control the number of radiations. These radiations enter the interferometer, where spectral encoding is performed after the beam falls on the sample, which is further either transmitted through or reflected off the material's surface. The final measurement is done in the detectors, which are mainly designed to measure the interferogram signals. The measured signal is then sent to the computing platform where the mathematically intense Fourier Transformation is done, and the Infrared spectrum is formed
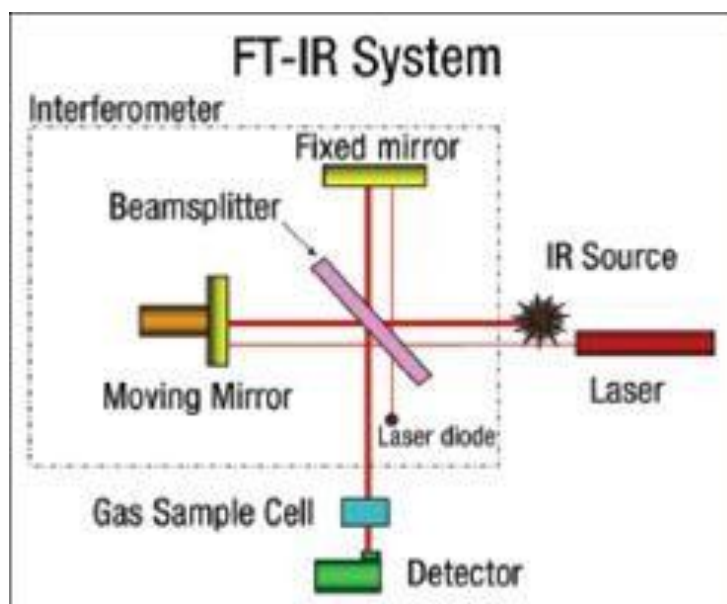
Figure 0-5 Principle of FTIR spectroscopy

Each bond in the samples exhibits different frequencies the same bond in two different molecules have a different environment in their surroundings so they absorb two different frequencies in the molecules spectrum. The absorption spectrum is an image of the bonds present in the molecules. The spectrum is calibrated for each specific bond when we detect the peaks and compare it with the calibrated peaks we get the desired results if not then we can find the drawbacks during synthesis whether the sample is correct or not.[9]

The basic working principle of Fourier transform infrared spectroscopy is the time domain is converted by using mathematical relations into the frequency domain [10].

1.6 Scanning Electron Microscopy (SEM)

A high-energy beam of the electron is used for the structural analysis of samples in powder, pellet, and thin-film forms. When a high-energy beam is irradiated over the sample the electrons interact with the surface of the samples and bounce back. The back scattered electrons confirm the structure of the sample. The structural information includes surface morphology, size of particles, shape geometry, and crystalline structure. The size from 1cm to 5 microns can be measured and the

resolution power is about 300000 times. The images can be seen up to 50nm easily by using SEM [11, 12]

When electrons are irradiated over the surface of samples the electron bounces back in three categories secondary electrons, backscattered electrons, and phonons which are characterized by the XRD for EDS analysis[13]

Electron microscopy consists of the following main parts

- Electron gun
- Secondary electron detectors
- Magnetic lenses
- Sample stage

Scanning electron microscopy was used to study the sample of barium titanate. Different operating voltages were used to take SEM images of Barium titanate. The schematics of SEM images are given as follows [14].

Backscattered electrons originate from a broad region within the interaction volume. They are a result of elastic collisions of electrons with atoms, which results in a change in the electrons' trajectory. Think of the electron-atom collision as the so-called "billiard-ball" model, where small particles (electrons) collide with larger particles (atoms). Larger atoms are much stronger scatters of electrons than light atoms, and therefore produce a higher signal (Fig.2). The number of the backscattered electrons reaching the detector is proportional to their Z number. This dependence of the number of BSE on the atomic number helps us differentiate between different phases, providing imaging that carries information on the sample's composition. Moreover, BSE images can also provide valuable information on crystallography, topography and the magnetic field of the sample.

Secondary electrons come from within a few nanometers of the sample surface, with a lower energy compared to the backscattered electrons. They are very sensitive to surface structure and provide topographic information. Secondary electrons, originate from the atoms of the sample: they are a result of inelastic interactions between the electron beam and the sample.
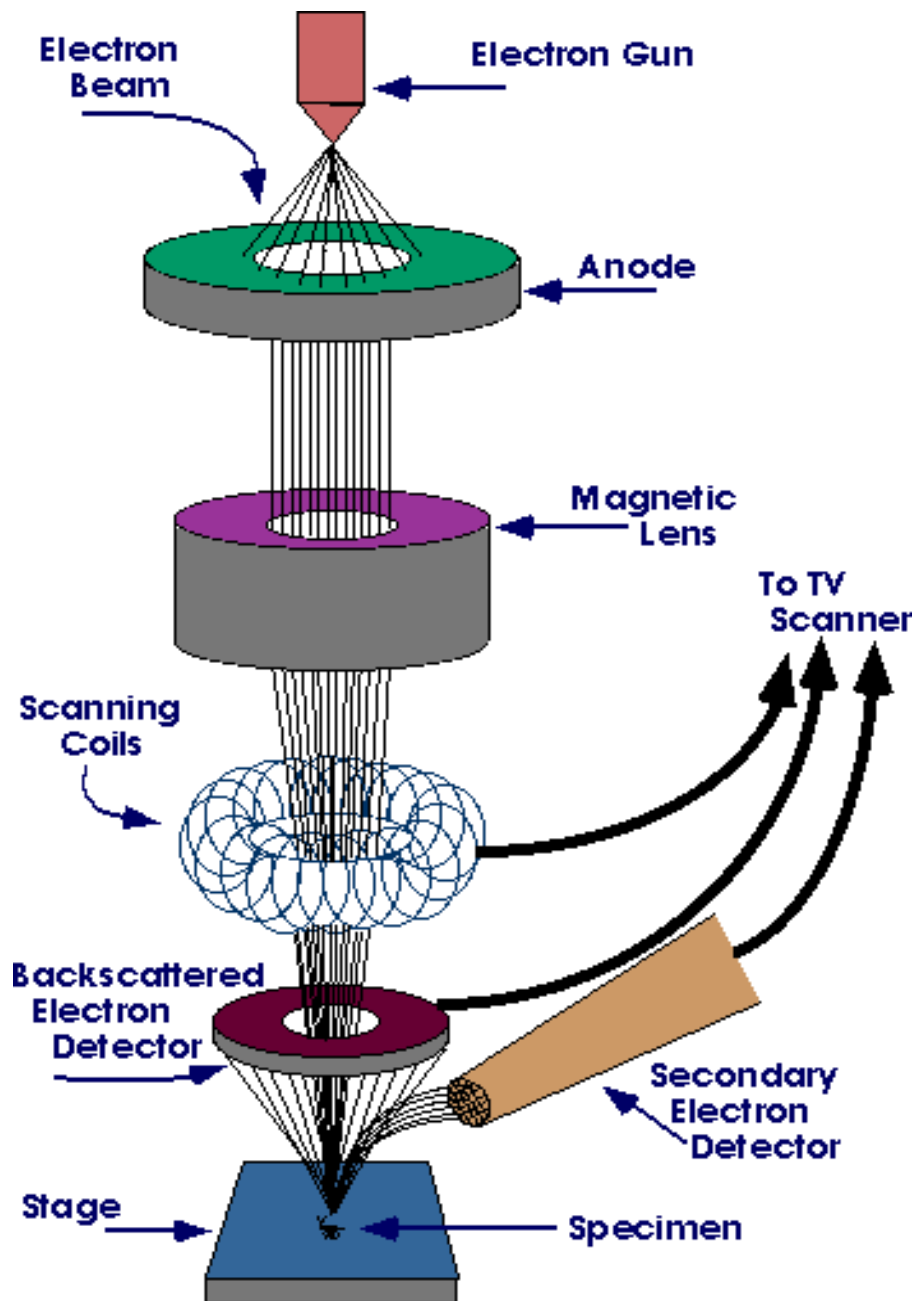
Figure 0-6 Scanning electron microscopy (SEM)

These characteristic X-rays are produced when electrons hit the sample surface. They give information about the elemental composition of the sample.

1.7 LCR Meter:

LCR meter is an electronic component used to measure electrical properties. Which is used for the electrical testing of dielectric materials and pellets. The LCR meter measures the Inductance, capacitance, and resistance of electrons [15]. The impedance analysis can be carried out by using an LCR meter or displaying the LCR meter converts impedance to the corresponding values of capacitance and inductance. The AC source is applied to the sample under test to measure voltage and phase angles between voltage and currents. By knowing these values we can find out the impedance.

Figure 0-7 LCR Meter

1.8 Breakdown Strength

The breakdown strength of the material is found to know the maximum voltage it can withstand without failure. The breakdown strength values were obtained and analyzed.

1.9 Dielectric study

The dielectric study enables us to understand the dielectric properties of ceramic materials, such as tangent loss, deficiencies found in the material, its nature, and the kind of polarization. As discussed in the literature review that polarization has many types it can be (ionic, electronic, orientation and space charge polarization) or

relaxation process. The dielectric constant can be carried out by using a mathematical relation

$$\varepsilon = C_P \, d \, / \, \varepsilon_0 A_r$$

Where

C_P = the parallel capacitance d = thickness of pellets

ε_o = permittivity of free space A= area of the pellet

When pellets are subjected to an electric field at different frequencies the polarization is built up inside the materials all types of polarizations can build up inside the sample. This gives us the dielectric loss represented as tan δ. When the temperature rises both factors dielectric loss and dielectric constant increases whereas both factors show a decline in the graph with rising frequency. The deviation trend usually occurred with temperature and frequency confirms the behaviors of the compound is a dielectric material

There are two main mechanisms in the dielectric study

(1)   Lowering the frequency and rise in temperature
(2)   Higher the frequency with the rise in temperature

In the first mechanism at lower frequencies the dielectric loss and tangent loss, both factors show an increasing trend this is due to the build-up of space charge

polarization inside the materials with increasing temperature. The tangent loss is increasing due to the release of space charge polarization in materials. [17,18]

The second mechanism can be understood well by the Maxwell Wagner model and Koop's model. This model explains that dielectric materials are constructed with the conducting grains and grain boundaries. The conducting grains are dominants at higher frequencies and grain boundaries are effective at lower frequencies. The electron transfers through grain boundaries and conducting grains. The grain's boundaries are very highly resistive and electrons accumulate at the boundaries at lower frequencies and give rise to the dielectric constant. Similarly, at higher frequencies, the electron changes its direction so vigorously the hoops model doesn't

match with the frequencies as a result dielectric loss decrease.

1.10 Impedance analysis

The impedance analysis is a very effective technique to check out the electrical and dielectric response when different ranges of frequencies are introduced into a material. To measure the output response of samples with different frequency ranges an AC signal is applied to a specimen. Impedance is classified into two main parts Real part and the Imaginary part denoted by Z^R and Z^{IMG} respectively.[19,20]

The AC impedance can be measured by the following mathematical expressions.

$$Z = R + jX$$

$$Z' = R = |Z| \cos\theta$$

$$Z'' = X = |Z| \sin\theta$$

1.11 Comparisons of real and imaginary parts
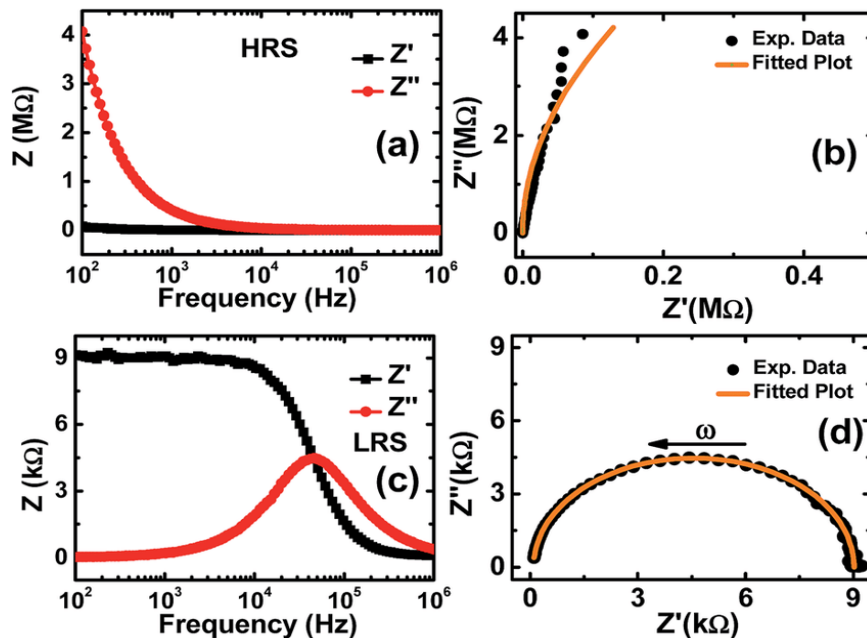
Figure 0-8   Real and imaginary part with frequency

1.12 Maxwell Wagner model

The Maxwell Wagner model is explained as the accumulation of charge at the interface between two materials. It is also applicable on micro to Nano level of the materials and molecular level.

1.13 Koop's theory

In Koop's theory, the grains are highly conductive but the grain boundaries are very resistive. When an electric field is applied the charges face the resistance at grain boundaries and this led a charge accumulation at the interface resulting from the interfacial polarization when frequencies are enhanced to a certain limit the electronic exchange occurs in ions and the real part of the dielectric constant shows the decreasing trend due to this mechanism.

1.14 Dielectric and Electromechanical Properties:

1.14.1 Dielectric Properties:

The LCR meter bridge is used to determine dielectric properties such as Dielectric loss, dielectric constant, tangent loss, electric modulus, etc. The capacitance of pellets finds out by using an LCR meter, and for dielectric constant calculation following formula is used.

$$\varepsilon' = \frac{C*d}{\varepsilon 0 A}$$

A represents the cross-sectional area of the pellet, C represents the capacitance, d represents the thickness, and ε_0 is the permittivity constant of free space and its value $8.85418782 \times 10^{-12}$ F/m. The imaginary part that corresponds to energy dissipation losses is calculated by using the following relation.

$$\varepsilon'' = \varepsilon' + D$$

There are some power losses in dielectric material due to friction, damping, and dissipation of charges during the movement of charges. The tangent loss factor and D- factor are expressed mathematically.

$$\textbf{Tan}\delta = \textbf{D} = \frac{\varepsilon''}{\varepsilon'}$$

AC conductivity of material calculated at room temperature by using

$$\sigma_{ac} = \omega\ \varepsilon_0\ \varepsilon''$$

1.15 AC impedance Spectroscopy:

The AC impedance parameters of pallets were measured at room temperature, resistance (R), and reactance (X) were measured at a frequency range over 100Hz to 5 MHz The impedance is a complex quantity that has two main parts, a real one and an imaginary. The imaginary part explains the fundamental element and reactance that give resistance. The relation is expressed as the real and imaginary parts of impedance in circuit relation Literature Review

Chapter No 2

Electrical Ceramic

2 Electrical ceramics

Ceramics materials have very versatile electrical properties. Some materials are known as an insulator which does not allow electricity even in a very strong electric field thus, they are excellent insulators. Some materials allow electricity passage without any alteration in a material known as excellent conductors but some materials require alteration for the passage of electricity in other words, we do band tuning and apply many other techniques to make them semiconductors, so-called doping. However, some ceramic materials do not allow electricity passage but when we placed them in an electric field they exhibit polarization and can be used in capacitors for electrical charge storage some of the electro ceramic materials that have been used are given as follow [21,22]

- Varistors are being used by Zinc oxide
- PZT materials are being used with Lead zirconium titanate.
- Capacitors are using with barium titanate materials
- For gas sensors, Tin oxide is introduced into the sensors
- For Opto-electric devices lithium Niobate
- Lead lanthanum zirconium titanate (PLZT)

2.1 Dielectric Materials

Good insulators are those materials that do not allow electricity passage and they are inert to the electric field but when we apply electricity to them they show some charge imbalance or slightly charge shift resulting in creating a dipole moment due to charge separation by electrodes or plates which gives the electrical polarization within the materials. Electrical polarization arises from the creation of dipole moments created by the individual atoms inside the domain walls with the increasing dipole moments electrical polarization also increases this phenomenon is known as

polarization. [23,24]

The applied electric field is directly proportional to polarization or vice versa

$$P = \varepsilon_0 \, \chi_e \; \ldots \; (2.1)$$

Where χe is the dielectric susceptibility, it has no unit it's a unitless quantity only describing dipole moment [M. Allison, 2007]. Since the dielectric susceptibility χe is equal to (εr-1), where ε_r shows the relative permittivity, the polarization is given as

$$P = \varepsilon_0 \, E \, (\varepsilon r\text{-}1) \; \ldots \; (2.2)$$

the molecule situated inside the dielectric material and between the plates experiences more electric field than inside the dielectric material resulting in the local field given as follows therefore called the local field (E_{loc}). The local field is induced in molecules and creates dipole moments that is given by [25,26]:

$$P_{mol} = \acute{\alpha} \, E_{loc} \; \ldots \; (2.3)$$

Hence P_{mol} depicts the moment and $\acute{\alpha}$ is the physical representation of polarizability. The overall dipole moment is defined as N number of molecules per unit volume known as dipole moment or polarization.

$$P = N \, \acute{\alpha} \, Eloc \; \ldots \; (2.4)$$

Putting equation (2.4) in equation (2.2) :

$$(\varepsilon r\text{-}1) = P/ \, \varepsilon o \, Eloc = N \, \acute{\alpha} \, Eloc \, / \, \varepsilon o \, E \; \ldots (2.5)$$

Polarization is very versatile it can be ionic polarization, orientation polarization (dipole) polarization, and space charge polarization. [27]
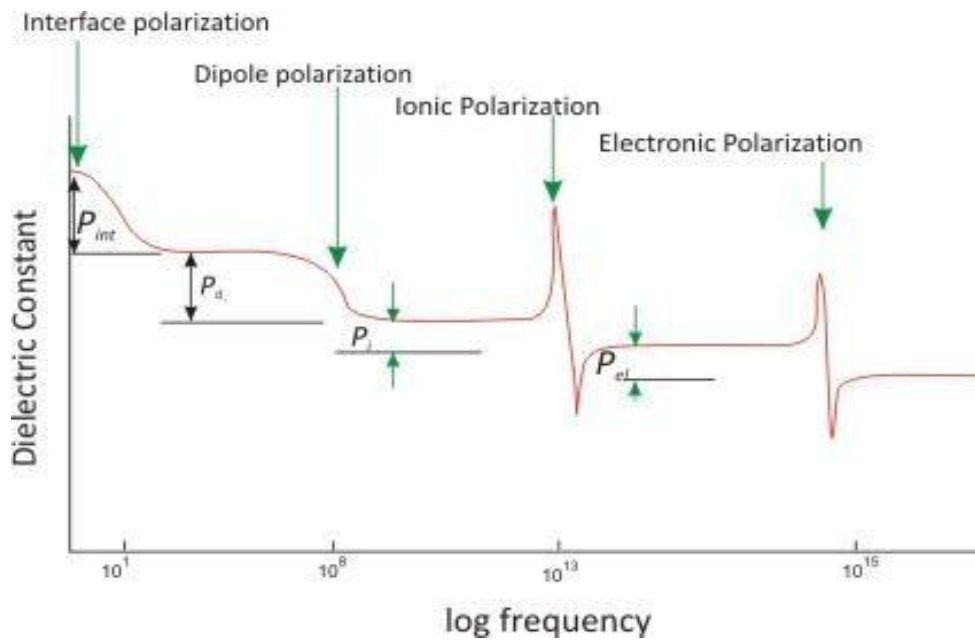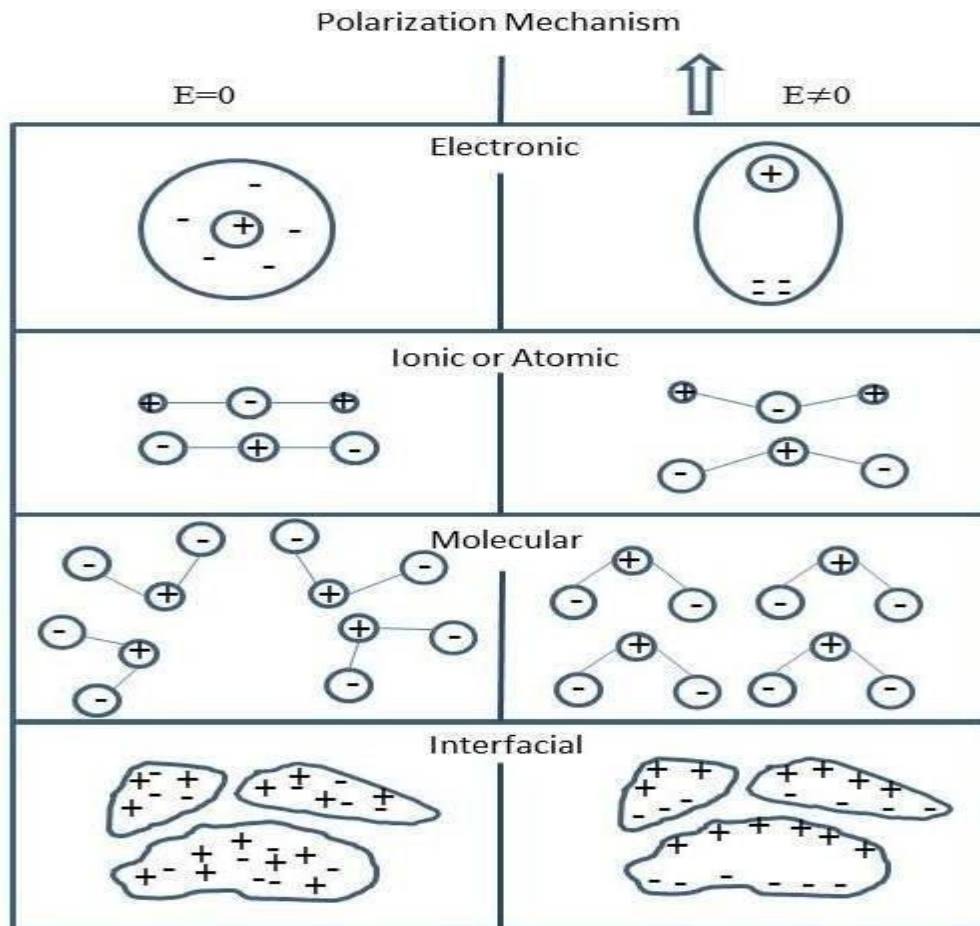
Figure 2-1 Types of polarization mechanisms

2.2 Electronic polarization

Those dielectric materials in which electronic polarization occurs when subjected to an electric field the electronic clouds in the atoms slightly shifted towards the positive electrodes and the nucleus having a positive charge slightly shifted toward the negative electrode creating. Dipole moment in the material $P = ά E$, where $ά$ represents the polarizability of the atoms. When the electric field vanishes the polarization within dielectric material disappears at this instant this mechanism is for a very small time as compared to other mechanisms. [28,29]
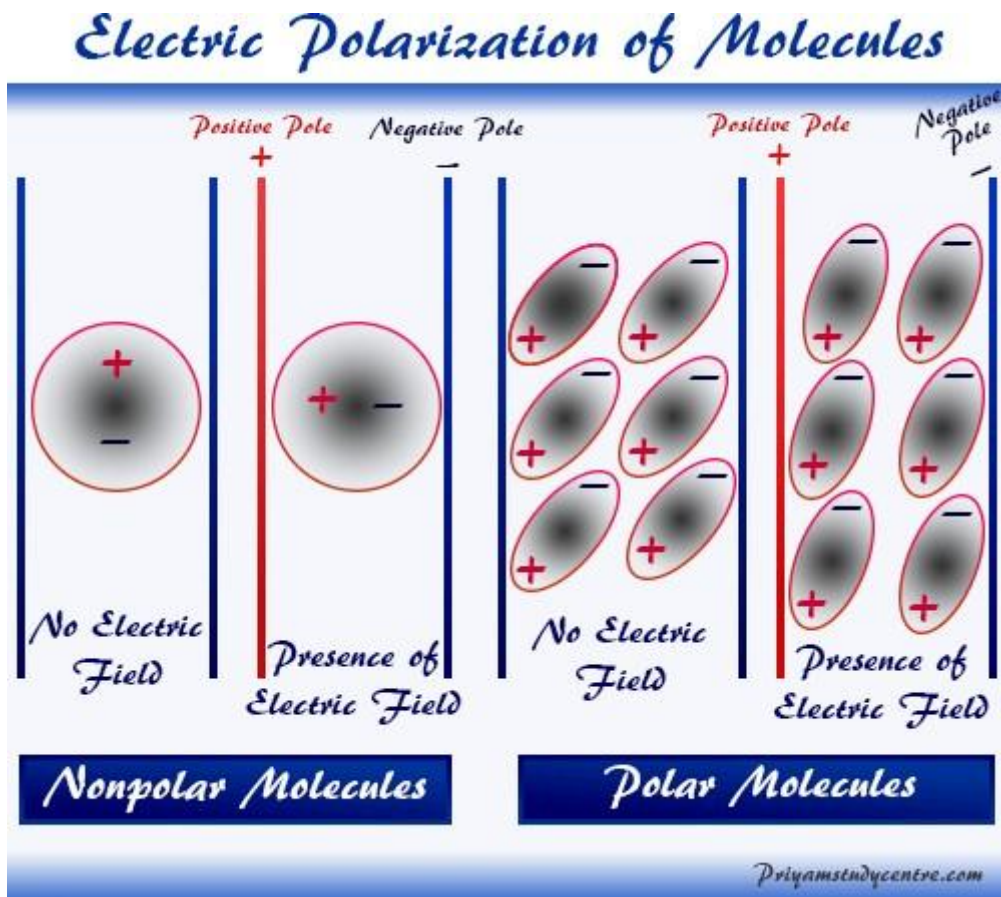
Figure 2-2 Electronic polarization

2.3 Orientation polarization

Some materials are made up of different types of atoms and interconnected by bonds with each other. The arrangement of atoms is different in different molecules for

Example H_2O, HCl, CHBr, Hf, and C_2H_5 (NO_2). For H_2, the arrangement of covalent bonds is such that the two hydrogen atoms have a net negative charge toward the oxygen atom. Inside the materials, one side is toward the positive electrode. CO_2 is non-polar because its atom is covalently bonded linearly. H_2O is watering its molecules arrangement or bond arrangement is triangular.

In large molecules, a large displacement occurs as a result of a higher polarization value because the distance between nucleus and electron is much higher than individual atoms. In solids, atoms are very tightly bound with each other but in liquid and gases they are very loosely bound so this effect has great importance in liquid and gases rather than in solids as the lower the temperature, the thermal vibration decrease, and as a result, it gives rise to dielectric constant. [30]
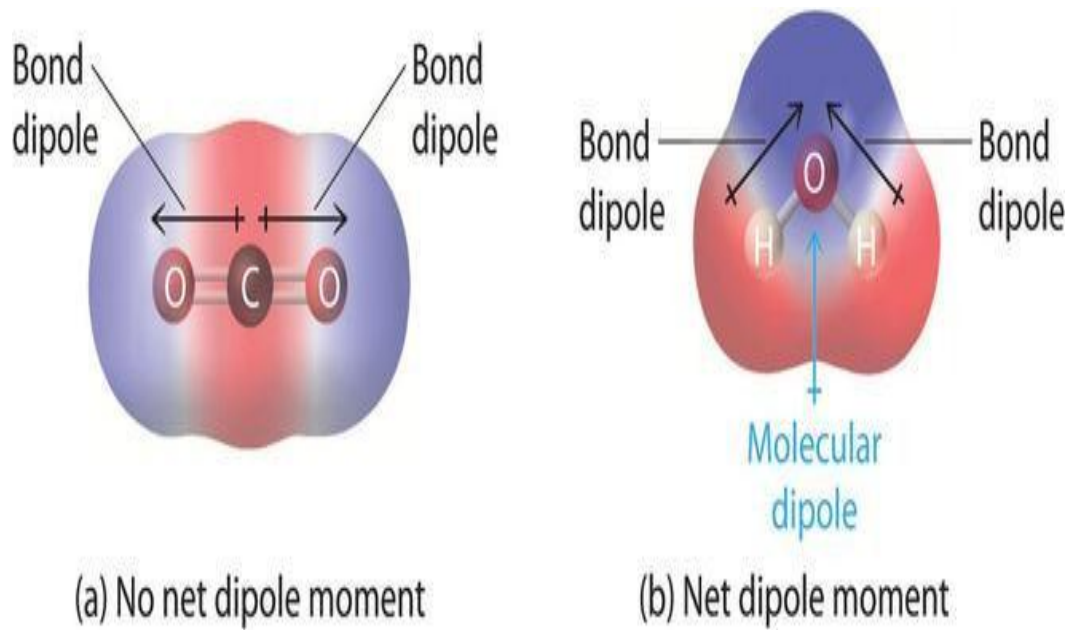
Figure 2 b) Shows the dipole trend as polar and non-polar   (a) (b)

2.4   Space charge polarization

Space charge polarization is also known as interfacial polarization. It is defined as the separation of positive and negative charges inside the material which are freely moveable when the external field is applied to it they form space positive and negative charges in the bulk of materials.

2.5 Atomic or ionic polarization

Atoms and ions are displaced from their original position when they are subjected to an electric field this is due to the stretching of bonds between them this stretching will cause the moment among the molecules of materials. This movement of ions and molecules creates atomic polarization in the materials. This mechanism is used for a wide range of polarization depending on many factors like solid solution and crystal structure.
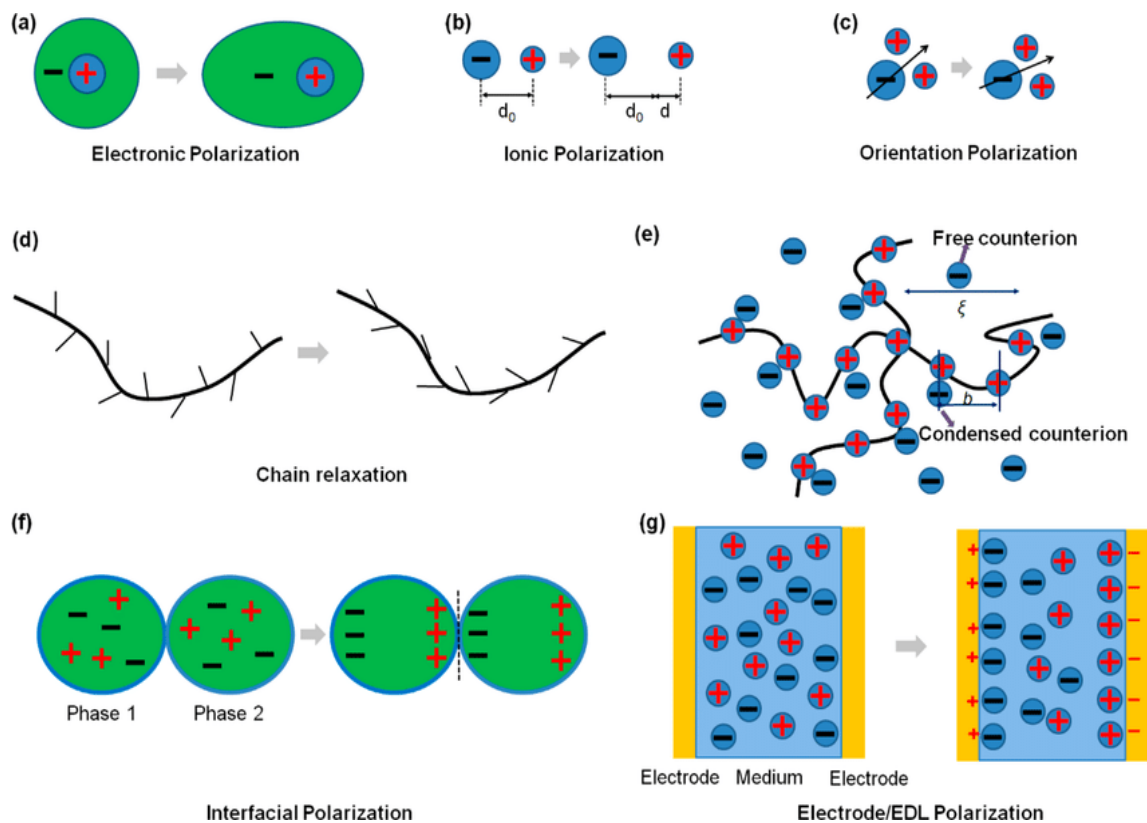
Figure 2-3 Polarization mechanisms

2.6 Dielectric Constant

The property or the charge storage ability of dielectric materials is known as the dielectric constant.

$$k = k \text{ mat} / k \text{ vac} \quad (2.6)$$

ε represents the relative permittivity while ε_o represents the relative permittivity of free space its value is 8.85*10-14 farad/cm (2.7).

$$\varepsilon_r = \varepsilon / \varepsilon_o \quad (2.7)$$
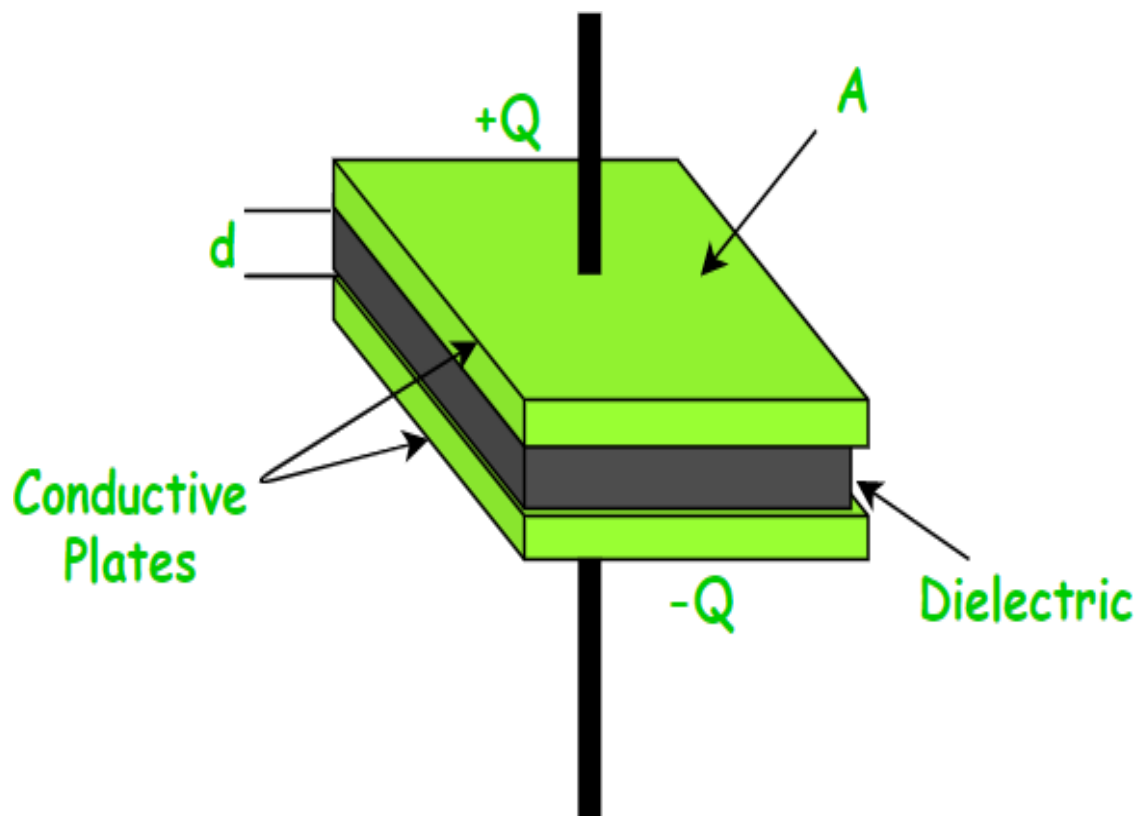
Figure 2-4 Polarization mechanisms

Some materials are having very low dielectric constant and used for the applications demanding excellent insulators. Some materials have very high dielectric constant and they are using as storage devices in electronic industries and, for the fabrication

of many electrical components. We can modify the dielectric constant with temperature. Polarization depends upon the source of polarization. Ionic or atomic polarization is intensive to temperature while molecular polarization is inversely proportional to temperature as temperature increases the polarization goes decreases the dielectric constant can be changed by variation in frequencies source, different frequencies have different dielectric constant or other electromagnetic sources irradiating on the materials. Electronic polarization increases with frequencies very rapidly, for example, visible light has great potential of frequencies of approximately 1015 cycles per second and has a direct impact on polarization.

Molecular polarization only responds to low frequency in higher frequency ranges molecules cannot align themselves with time with each cycle.[31]

2.7 Dielectric Loss

Ideal capacitors don't allow any type of charge flow it permits only displacement of charge via polarization, voltage lags by a 90-degree angle, or in other words current leads the voltage by the angle of 90 degree which is out of phase in reality real materials always gives some loss because the phase angle between the current and voltage is not 90 degree exactly it's lag behind to some extent so-called power loss

$$\textbf{Power loss} = \pi f \textbf{ V 2 } \varepsilon \textbf{ tan } \delta \textbf{ ....(2.8)}$$

The term "ε r tan δ" is the physical representation of the loss factor. The loss factor tells us about the class of material in both cases insulator and dielectric materials. This loss factor is also termed tangent loss or dissipation factor. In both cases, low power loss is required

The dielectric loss is dependent on the following term.

- Ion migrations

- Ion vibration and deformation

- Electronic polarization

Temperature and frequency have very strong effects on ion migration. With the

increase in the temperature and lowering the frequency the dielectric constant increases. Another main thing is overheating or cycling heating which alternates the results of dielectrics which results in the degradation of dielectric and breakdown strength. Rating of dielectric materials involves the following terms

- Relative permittivity
- Tangent lag angle
- Dielectric constant

2.8 Dielectric Strength

Dielectric strength is an intrinsic property, it is defined as the ability to bear and withstand with external electric field without the passage of electric current through the material Dielectric strength appears when a high electric field is applied to the material and electrons get enough energy to jump into the conduction band and accelerated with high energy. Some of the electrons transfer their kinetic energy to the valance band electron and these electron transfer into the conduction band when a large number of electrons jumps into the conduction band an avalanche of electrons is loosed and the current flow very rapidly through the dielectric material this process damages the dielectric material by melting or burning of dielectric materials.

This process is initiated by the conduction of electrons. There are several mechanisms of this process or in several ways, they may originate. The most common way is the contaminated surface of the insulator and the arching between high potential lead impurities atoms can also provide electrons during this process and pores in materials provide channels creating gas discharge. In conventional capacitors, the dielectric materials burn or melt at relatively low field strengths when mechanical and chemical abuses occur and also when subjected to very high electric fields for a very long time.[32]

Some other properties exist in dielectric materials piezoelectricity, pyro-electricity, and ferroelectricity. Piezoelectricity is the intrinsic property of the material. Piezoelectricity is a stress-dependent property when stress is applied to the material the physical changes occur in a material having a single crystal. The alternating

current (Ac) and voltage changes occur. There are 32 classes of piezoelectric 20 of them are piezoelectrics materials. Some directions of crystals are piezoelectric some may not when this type of material is placed in an external electric field the reverse process takes place in that material.

Pierre and Jacques firstly discovered the piezoelectric effect in 1880 piezoelectricity are naturally occurring property identified by Pierre and Jacques. Some laboratory-grown materials are also having these properties for example quartz, zinc blende boracite, and sugar. The widespread use of piezoelectric devices in phonograph picks up, microphones, accelerometers and sonar devices.

2.9 Piezoelectricity

Piezoelectricity is the property of a material that gives the changes in properties alternating current or voltage changes in the material when stress is applied. Some materials which are usually known as single crystals or anisotropic materials show charge imbalance when stress is applied to this type of material its drives net positive and net negative charges on alternative sides. Piezoelectric materials are those materials that are anisotropic (there are a total of 32 crystal classes found in materials among these 20 are known as piezoelectric materials). There is a problem that all of them are not piezoelectric in all directions these crystals show shape variation when subjected to external voltages. The piezoelectric effect is firstly introduced by Pierre and Jacques in 1880. Some materials are natural and some of them are laboratory- grown single crystals. The names of laboratory-grown materials are Zinc Blende, quartz boracite, topaz, and sugar-potassium tartrate tetrahydrate are some common examples ($NaKC_4H_4O_6.4H_2O$). Due to these piezoelectric effects, these materials are introduced for the fabrication of many electronic components and made this material very innovative for sonar devices, sensors, phonograph pickups as well as in accelerometers. [33,34]

2.10 Pyroelectricity

Some materials having the property of being naturally electrically polarized are known as pyroelectricity when the temperature changes the voltage changes occur inside the crystals the temperature slightly shifts the position of atoms such that the position of atoms changes when they are cooled or heated. The polarization changes give the voltage changes across the crystals if the temperature within the crystal remains for a long time inside the crystals the polarization disappears after sometime this is due to the leakage current. The leakage can be due to the movement of electrons or ions.

Pyroelectricity can be seen as the sides of triangles representing kinetic, thermal, and electrical changes. The side between the electrical and thermal are pyroelectric and produces no kinetic energy. Similarly, the side between the kinetic and electrical corner produces no heat effects. [35,36]

2.11 Ferroelectricity

Ferroelectricity is analogous to Pyroelectricity with the additional property there is naturally spontaneous polarization present inside the material in which an electrical field can reverse the polarization effect.

Ferroelectric material exhibits non-zero spontaneous polarization even after the applied electric field. Strong electric fields can reverse the direction of polarization which shows the phenomenon just like hysteresis loops same as in ferromagnetic materials. The ferroelectric is also called analogous to ferromagnetic materials due to its spontaneous magnetization effect and gives a similar graph of hysteresis loop as in ferroelectric materials. These materials reveal the ferroelectricity only below the phase transition temperature. This temperature is known as Curie temperature [37]. When the temperature reaches T_C it transforms into Paraelectric materials where spontaneous polarization vanishes and becomes zero after curie temperature it becomes the paraelectric materials.

Ferroelectric materials can be used in capacitors because we can adjust the capacitance of capacitors. The ferroelectric materials are sandwiched between the electrodes. The permittivity of ferro electricity is not only high but can be tuned or

adjusted especially when the temperature is near to its curie temperature. The size of capacitors having ferroelectric materials is relatively small as dielectric nontune able capacitors of similar capacitance.

Ferroelectric materials are introduced in many electrical components for Sensors. Sensors may be vibration sensors or may be fire sensors and as a fuel injection in diesel engines. These sensors are used on a very large scale and have widespread usage across the world [38,39].
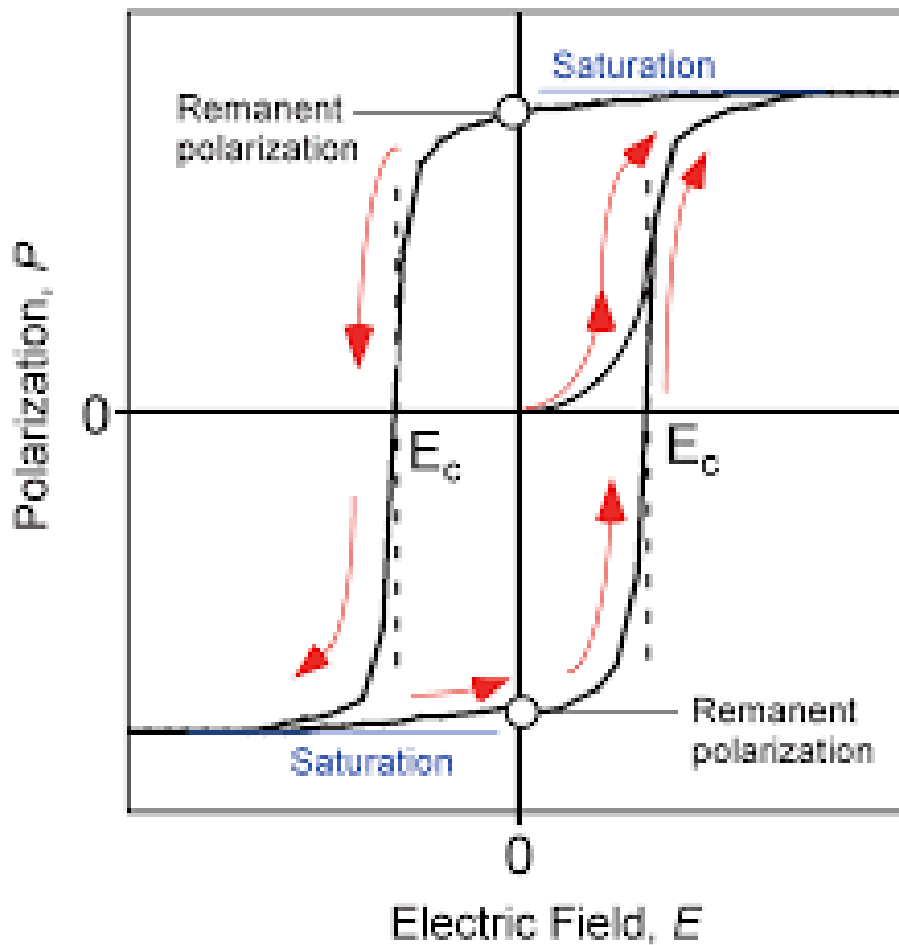

Figure 2-5 Ferroelectric polarization

2.12 Ferroelectric Materials

Most of the ceramic materials which have been synthesized with ferroelectric properties are utilized for many useful applications. Among this family many materials have a structure so-called pervoskite structure generally represented by ABO_3. This structure is very desirable. In the barium titanate ($BaTiO_3$) Lead titanate ($PbTiO_3$) and lead lanthanum zirconate titanate (PLZT) are having a pervoskite structure. A brief account of some of these materials is given in the following sections. [40]

2.13 Literature review

2.13.1 Lead Titanate ($PbTiO_3$, PT)

Some materials exhibit the same properties due to their structure similarly the lead titanate has a structure like barium titanate $BaTiO_3$. Its curie temperature is 450 degrees. With the decrease in the temperature below Curie temperature, there is a phase transition from paraelectric cubic to ferroelectric tetragonal phase. The lead titanate vessels are very difficult to make because below curie temperature changes its phase from cubic to tetragonal to $PbTiO_3$ and cracks appear during processing. The automatic stiffness takes place when it becomes cool, it can be reduced by the addition of various dopants. Some dopants named Ca, Ba, and Sn get a crack-free structure.[41]

2.13.2 Lead Zirconate Titanate {Pb (ZrxTi1-x) O3,PZT}

PZT is the most popular piezoelectric ceramic material. PZT also has a perovskite structure in each unit of divalent metal ions with a large lattice generally holding small tetravalent ions. PZT the small tetravalent ions are mostly zirconium or titanium and the divalent ion is lead in the lattice.[42]

PZT behaves in both senses when it deforms it produces an electric charge inside the material this property is called the piezoelectric effect similarly when an electric field is applied it shows deformation, which is the inverse process of this property called the inverse piezoelectric effect. Piezoelectric materials are its best choice due to their chemically inert nature, stable material, and inexpensive to synthesize. It can be modified easily to meet the required properties for desired applications. Another

important feature of PZT is that they have very high sensitivity and can be operated at higher temperatures rather than other ceramics. PZT materials are used in ultrasonic cleaners and sonar devices. PZT is mechanically very stable it minimizes the effect of mechanical loss and enables it at lower operating temperatures. It has also a low dissipation factor. PZT materials have high dielectric stability. [43,44]

2.13.3   Lead Lanthanum Zirconate Titanate (PLZT)

Lead lanthanum zirconate is an anti-ferroelectric material. When an electric field is applied it switches from anti-ferroelectric into ferroelectric material. This is accomplished by the large volume of expansion. This led it toward interesting material for applications of actuators. When structural changes occur in a material the unit cell parameters also change. This is significant to monitor the phase changes from Anti ferroelectric to ferroelectric materials. The compositional modifications in materials are also important for practical applications.[45]

The nitrogen is doped in lead lanthanum zirconate titanate by dopping of nitrogen the ceramics were made to inquire about the optical absorption of the material. For PLZT the UV/UV-VIS tests were performed and it has been seen that the optical absorption of doped PLZT is wider than the undoped PLZT. This phenomenon is important for the conversion of optical energy into electrical energy [46].

Similarly, another interesting phenomenon is seen that the doped PLZT ceramics materials emit photocurrent and photovoltage rather than undoped PLZT ceramics. Barium and strontium both were doped into PLZT for the modification of electrical properties it was examined that the electrically induced phase change for strontium decreases both the antiferroelectric and ferroelectric transition temperature and temperature of maximum dielectric constant.

Similarly, the addition of barium into PLZT causes temperature changes. It reduces the T_{MAX} (Dielectric constant) and increases the phase transition temperature.

2.13.4   Lead Magnesium Niobate (PMN)

Lead magnesium niobate is having a perovskite structure. It is important material because of its high electrostrictive strains and correspondingly high dielectric constant. Due to the formation of a stable pyrochlore phase, it is become very hard to synthesize in a polycrystalline ceramic form.

The single-phase lead magnesium titanate ($PbMg_{1/3}Nb_{2/3}/O_3$) was synthesized to study the dielectric properties it is concluded that with the addition of 10% $PbTiO_3$ for pure PMN dielectric constant is about 18000 and with PMN 31000 is accomplished. The

increase in dielectric properties is due to both increasing MgO and sintering temperature. The analysis confirmed the microstructure the increase is due to increasing grain size.[47]

2.13.5   Barium Titanate ($BaTiO_3$)

Barium titanate is the material that is used on a very large scale due to its high dielectric constant. because of the high dielectric constant, and remarkable ferroelectric and piezoelectric properties. The higher dielectric constant and excellent properties depend upon the crystal structure of the materials.

2.14   Methods of Preparation of $BaTiO_3$

2.14.1   Solid-state reaction method

In past years ago many other techniques are being used for the synthesis of $BaTiO_3$ but this chemical approach is used very frequently for barium titanate powder by mixing the powders. The precursors are mixed in ethanol $BaCO_3$ and TiO_2 at very high temperatures usually at 1100 degrees. With the advantages of the solid-state reaction method having a single and low-cost process, there are many disadvantages of this method. When the synthesized powder is Calcined at a higher temperature for solid-state reaction many issues arise in the powder for example agglomeration of powder, large particle size, and wide size distribution. This limits the fabrication of

electronic components so we need to improve this disadvantage to get the desired results [49].

To change the microstructure and sintering properties a mechanical activation is required called ball milling. It influences both of them. High-energy ball milling is generally used to mechanically activate the powder known as the mechanochemical process [50]

The mechanically activated powder has much higher sinterability than other conventional methods. The dielectric constant changes with the particles size changes [51].

Advantages:

- They were widely used to produce PZT powders because of their high yield, low cost, and simplicity.

- In PZT, with the evolution in high-energy milling technology, particle size below the micron level is achievable with good chemical homogeneity, and narrow size distribution can be fabricated easily.

Disadvantages:

- The broad size of particles, impure and inhomogeneous size of particles.
- Calcinating the mixture at high temperature increases the agglomeration loss of volatile oxides, e.g., lead oxide in PZT, and over the coast of the production.

2.14.2 Chemistry-based methods

Various chemical routes are being used for the synthesis of barium titanate powder. Every method has its advantages over the other methods, for example, the sol-gel process is a very popular technique for making a thin film, and the similarly hydrothermal method is a good technique for the synthesis of Nano particles based on the advantages and disadvantages researcher uses many techniques for the desired properties and applications some of the chemical routes are Sol-gel processing, Hydrothermal method, Spray pyrolysis and many other techniques are being used.

2.14.3 Hydrothermal method

The hydrothermal thermal method is usually a low-temperature technique in which autoclave and Teflon are required. Teflon is coated inside the autoclave to remove or to avoid the corrosion of chemicals on the side walls of the autoclave. The hydrothermal chemical approach is generally known as a good technique for the shape and size control of powders. Extensive studies have focused on the particle size and Composition of the phase for dielectric properties generally high sinterability and high dielectric constant is required. We can synthesize barium titanate hydrothermally under moderate conditions. [52]

Nano crystallite powder barium titanate is synthesized by using acylated titanium and barium acetate using a hydrothermal approach. This is top to bottom approach in which we touch the Nano-scale by using bulk materials. During the synthesis, the researchers study the effects of the molar ratio of precursors on barium titanate powder .it is found that particle size can be modified with reaction conditions some of the conditions are atmospheric pressure, temperature, and time of reaction which effects the particle size and shape as well. Two main areas are important in reaction kinetics the first step is nucleation and the second step is the growth of particles in the hydrothermal method.

Dissolution and precipitation are the formation mechanism of barium titanate via the hydrothermal route. The synthesized thin film of barium titanate is roasted over the single rutile crystal of TiO_2 under hydrothermal conditions impurities and other factors strongly affect the morphology and size of the particles.

Advantages:

- We can control the rate of reaction kinetics due to the temperature and pressure of the reaction

- The product obtained through hydrothermal reaction has good purity, composition, and morphology of the particles

Disadvantages:

- Maintaining the temperature and pressure of the reaction it is highly expensive

- Highly risky and accidental because of the reaction conditions such as high temperature and pressure.

Teflon coating is very necessary during the reaction of the hydrothermal method because the material coated inside the Teflon is resistive to the corrosive material used in reactions. Some chemicals are very corrosive in a reaction that damages the walls.

The schematic of the hydrothermal method is given as follows.
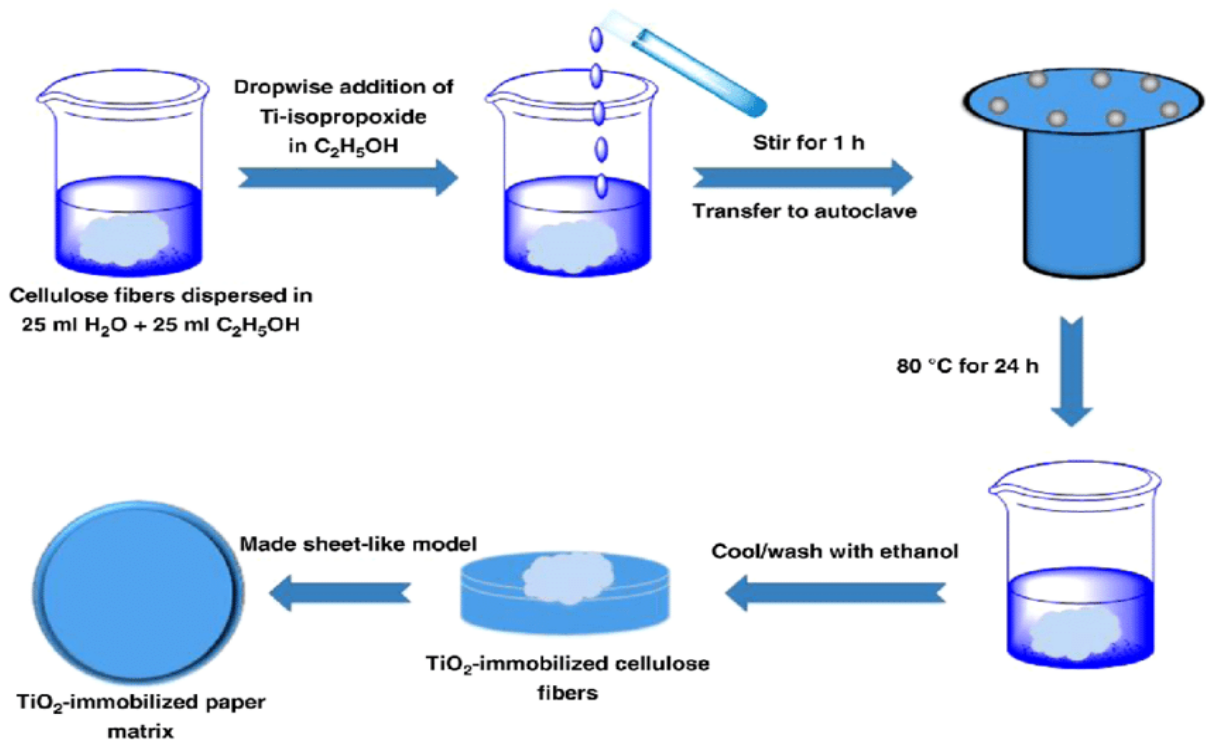
Figure 2-6 Schematics of hydrothermal method

2.15 Sol-gel processing

The sol-gel method is used for the synthesis and fabrication of thin films in electronic components. Sol and gel are two different terminologies. Sol and gel are formed during synthesis in two different steps firstly sol is formed in solutions when it dries it becomes a gel. The main processes are poly condensation and hydrolysis during the formation of a gel. By approaching the sol-gel route the synthesis of Nano powder of barium titanate with perovskite structure relatively at low temperatures. The following properties are being visualized during synthesis phase composition, particle size, micro structure, and phase ceramics. The sol-gel technique is mainly used for the coating process the composition can easily be controlled by this process like surface morphology engineering which permits the use of thermally fragile substrate several scientists and investigators are using this technique for the preparation of the thin film. [53 54].

Advantages:

- This process gives outstanding result with high purity of ceramics and controlled size of particles.

- By controlling the parameters of the reaction, we can manage the composition of the particles including all factors

Disadvantages:

- It is a complicated process with conditions and parameters.
- To achieve the desired chemical structure and morphology at higher temperatures with raw materials it is relatively expensive.
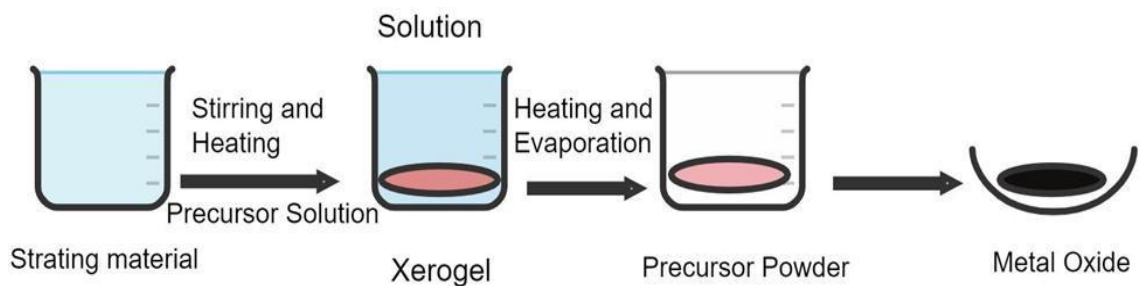

Figure 2-7 Schematics of sol gel process

2.16 Spray pyrolysis

The very well-known technique so-called spray pyrolysis is applied for the formation of barium titanate tetragonal structure by the combustion of metal nitrides. By precipitating barium titanyl oxalate {$BaTiO_3$ (C_2O_4)$_2$. $4H_2O$.} barium nitrate particles are synthesized. We convert these barium nitrates by spray pyrolysis into pure barium titanate [55].
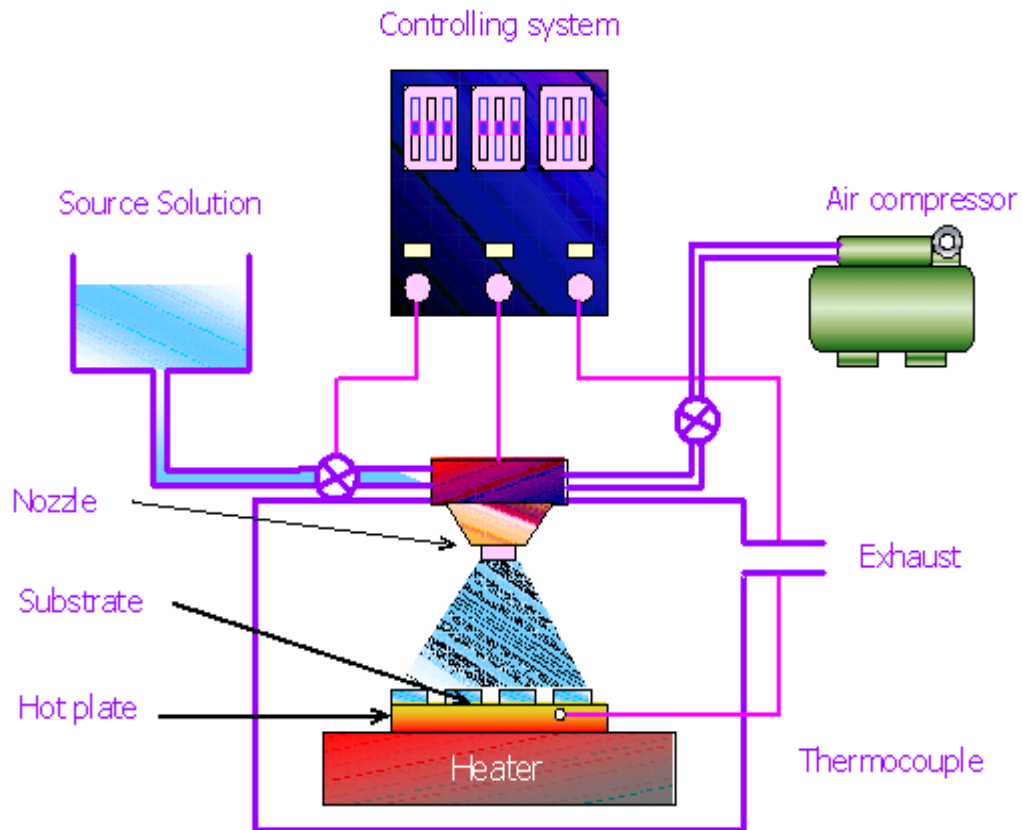

Figure 2-8 Schematics of spray pyrolysis.

Chapter no 3

Experimental work

3   Experimental Work

3.1   Materials for the preparation of BaTiO$_3$ powder

The materials used for the synthesis of BaTiO$_3$ were Barium Carbonate BaCO$_3$, Titanium Oxide TiO$_2$ powders. Both powders were of high purity to obtain high purity products. Barium titanate was prepared by solid-state reaction of the two raw materials using low-energy ball milling. The two powders were first measured to obtain a proper composition for forming BaTiO$_3$. Powders were then added to a plastic bottle. Zirconia balls of 1 and 3 mm in diameter were used to assure proper mixing. The balls were taken for about 20% of the total mixture to be formed. Ethanol (98% pure) was used as a mixing media. The powders were mixed in ethanol through low-energy ball milling for 24 hours at 200 rpm. A solution was formed after mixing, followed by drying at 75^{0}C in the oven for proper removal of the solvent. The sample obtained was then crushed in a gate mortar to obtain a fine powder. Calcination was carried out in a furnace for the removal of solvent for 9 hours.

3.2   Molar ratios

BaTiO$_3$	Cu Percentage %
1	0
2	5%
3	10%
4	15 %
5	20 %

The Calcined powder was carried out and dropped into an agate mortar for pellet making we started with crushing barium carbonate into a fine powder and then mixed with a polyvinyl so-called binder into powder. Polyvinyl binder is added in very less quantity for pellets making generally assumed to be 5 % in overall powder to get the desired form of pellets.

3.3   Drying in oven

The binder solution with powder is then dried in a microwave oven for 30 minutes because the binder is so viscous and stays wet for a very long time so we put the mortar in an oven to dry the powder. The dried powder is again crushed in a mortar for fine powder and dropped powder into a dye of 12 mm for pellet makings. The powder is pressed into dye by applying pressure in tons ranging from 1 to 5 tons for pellets. This pellet is then used for sintering in an inert atmosphere for 24 hours.

3.4   Inert atmosphere

Cu is when subjected to air at higher temperatures then it gets oxidized, we use the inert gases in a sintering machine called tube furnace by using argon and helium gases to avoid oxidization.

3.5   Precursors

Barium carbonate and titanium dioxide are the initial powders that were mixed in an equimolar ratio. When barium carbonate reacts with the titanium dioxide in ethanol its yield barium titanate

3.6   Ball milling

Ball milling process in which mixed powder in ethanol is placed onto ball milling roller. The solution appeared grey. It turns from white to grey. After ball milling, the solution is separated into a beaker for drying purposes

3.7   Microwave oven:

The mechanically activated powder after ball milling is placed in microwave oven

drying. The oven is adjusted to 90 degrees for the evaporation of alcohol. The boiling point of alcohol is 75 ^{0}C. It took 16 hours for the complete evaporation of alcohol. This process is repeated several times for each concentration of copper.

3.8 Grindin:

The dried powder is placed in an agate mortar for grinding. The main purpose of grinding is to convert it into fine powder for pelletization and sintering purposes.

3.9 Calcination:

The fine powder is placed into a heating furnace for calcination. The calcination is carried out for two hours at 900^{0}C. The heating rate was 5^{0}C/ min. This is shown in the graph
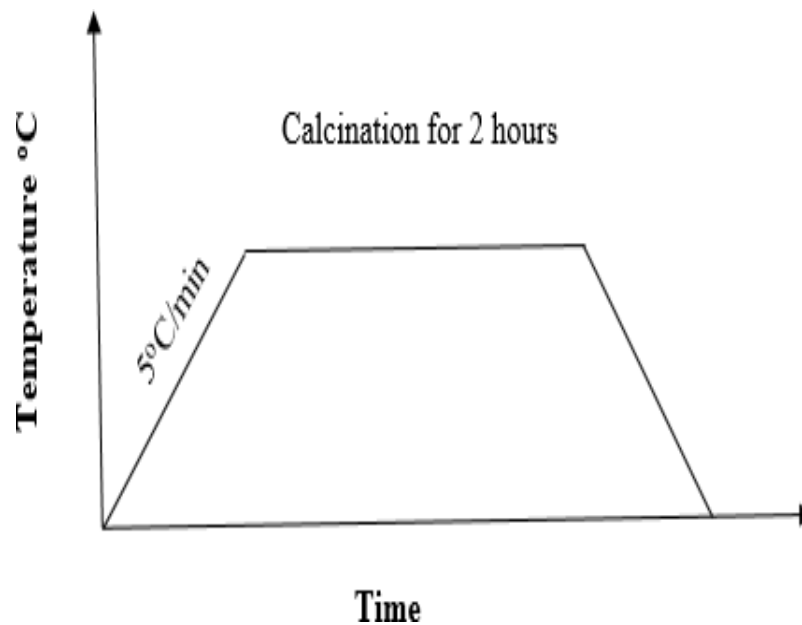
Figure 3-1 Calcination cycle

3.10 Addition of copper

Copper is added in different concentrations in Calcined barium for the synthesis of Cu-BaTiO$_3$ composite

3.11 Polyvinyl binder

The polyvinyl binder is then mixed into Calcined powder in very little quantities for pellet making. The binder is mixed and left for drying in Oven for 30 minutes. This process is repeated for all samples. The dried powder is dropped into a dye of 13mm for pellets and pressed on different pressure ranging from (1 to 5 tons). The obtained pellets were sintered out in a tube furnace.

3.12 Dielectric Property

3.12.1 Dielectric constant vs. temperature.

Dielectric tests were performed under the LCR meter at room temperature. All the synthesized pellets were pasted with silver from both sides to make good contact with the points of the meter. The temperature was adjusted at an interval of five minutes. Every 5 minutes the meter recorded the data with temperature to measure the dielectric constant. The temperature exceeded 150°C for the measurements of the dielectric constant. This process is repeated for five pellets with different concentrations of coppers.

3.12.2 Dielectric constant vs. frequency

This test is performed for five pellets with different concentrations of coppers. The frequency is gradually increasing while testing the pellets from 10^2 Hz to 10^6 Hz during testing. The meter recorded the data. This process is repeated for all the samples. The measured data is analyzed with the review papers and find out the results. We can find out the dissipation factors, tangent loss and dielectric loss of the materials. Capacitance, real part of impedance, imaginary part of impedance and Cole Cole plot of the obtained data. All the measured data is manipulated on excel file for the mathematical calculations and then measured the terms as discussed.
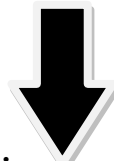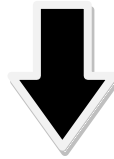
SCHEMATICS

**BARIUM
CARBONATE
(BaCO$_3$)**
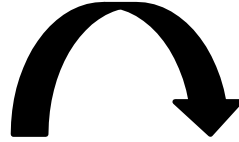
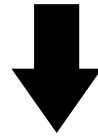**TITANIUM
DIOXIDE
(TiO$_2$)**

**Mixing in ethanol and
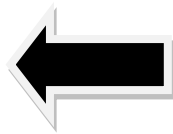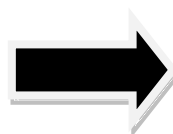ball milling for 24 hours**

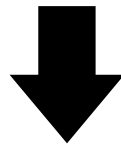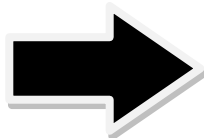**Drying in ovens at 90^{0}C
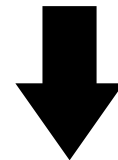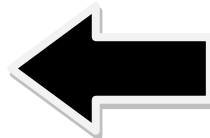for 16hours**

Calcination

Pellitization

SEM

Characterization

XRD

RAMAN

**DIELECTRIC
TESTING**

FTIR

Chapter No 4
Result and Discussions

4 Results

4.1 X-Ray Diffraction:
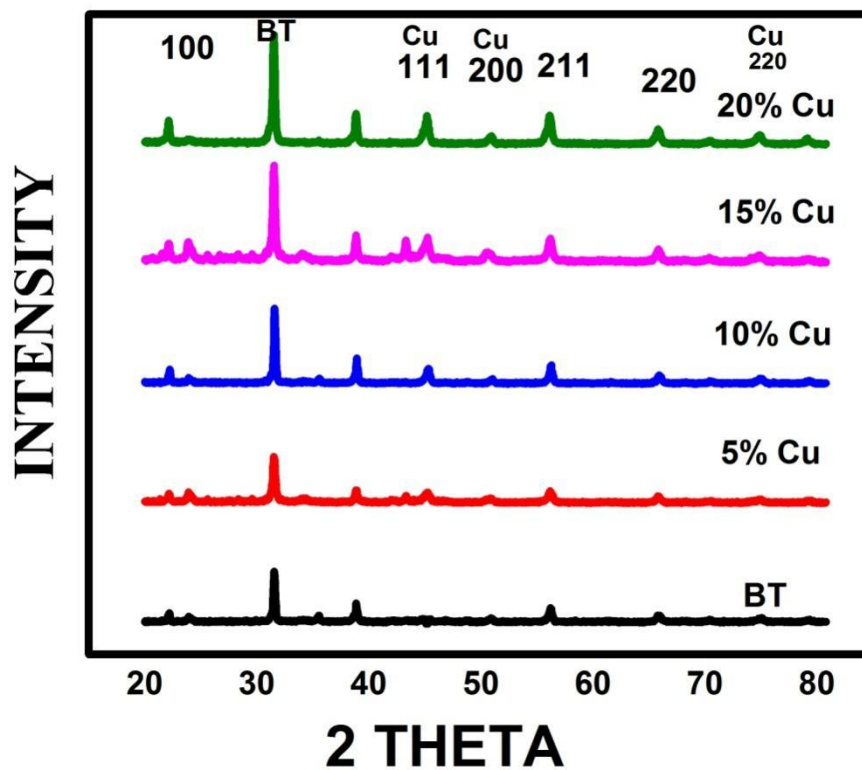

Figure 4-1 XRD of Cu- BaTiO$_3$ pattern

The XRD pattern of Cu-BaTiO$_3$ was measured on different concentrations of (Cu-BaTiO$_3$) ranging from (0 to 20%vol). All diffracted peaks were noticed which showed the Pervoskite structure of Cu-BaTiO$_3$ and there is no other peak is observed which determines the secondary phase and no other impurities are found during the XRD analysis. The detection limit applied is 0 to 90 degree. The major peak at (110) is the peak of Barium titanate which confirms the pervoskite tetragonal structure of prepared sample the copper peaks were observed at (200) planes. Which is the

major peak of copper (Cu) and the second and third peaks of coppers are at (111) and (220) planes. Sharp peaks confirmed the good Crystallinity and good tetragonal structure of the materials.

4.2   SCANNING ELECTRON MICROSCOPY (SEM)

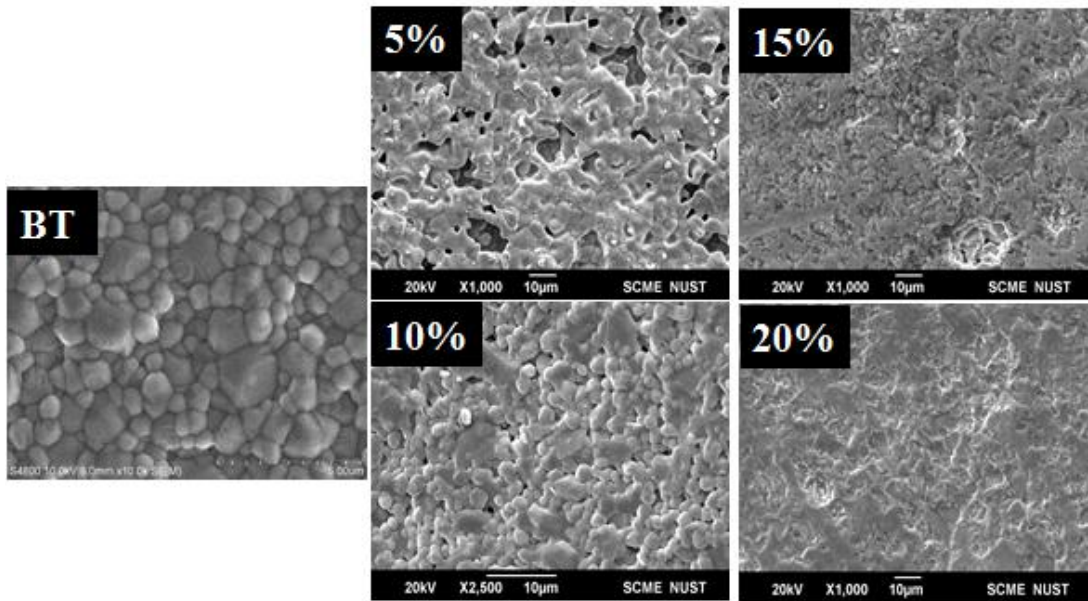Figure 4-2 SEM images of different concentrations of copper

With the addition of copper in barium titanate with different concentrations, SEM images are demonstrating the uniform and homogenous grains growth in the solid-state reaction method. The average grains sizes are 1 to 5µm. hence it is suggesting that undesirable products are inhibited by the solid-state reaction yielding pure products.
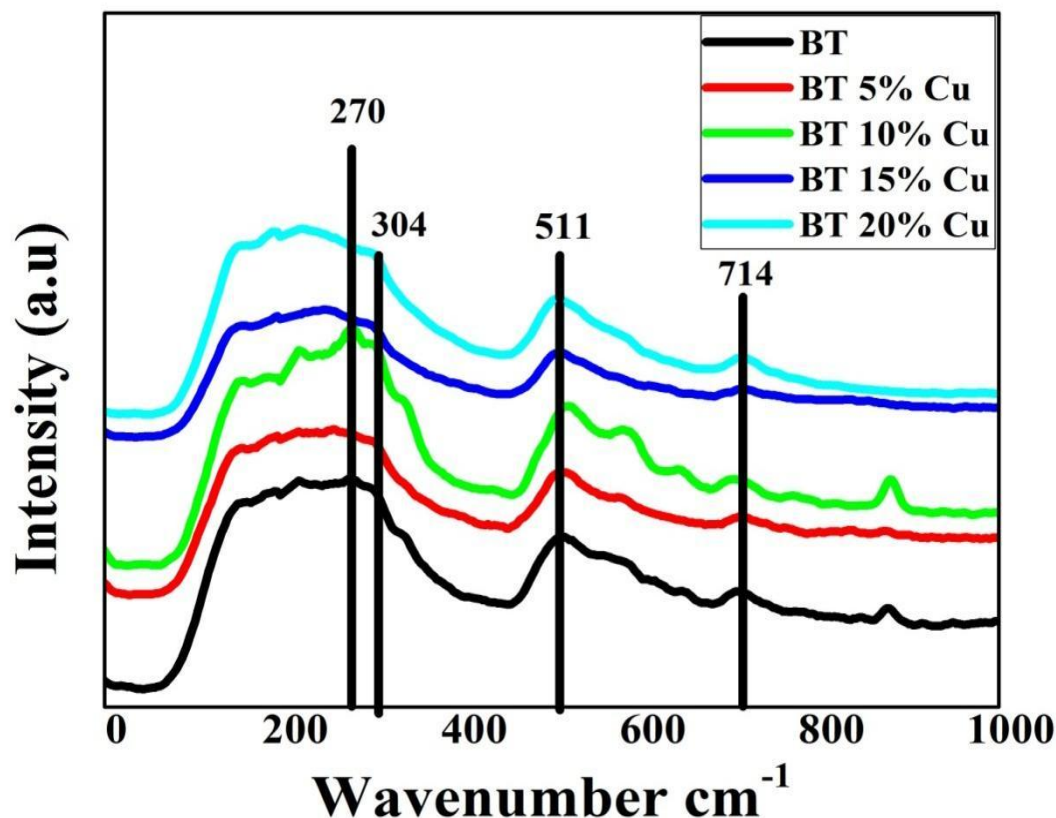
4.3 Raman spectroscopy

Figure 4-3 FTIR Spectroscopy

Raman spectrum of $BaTiO_3$ of calcined powder has different concentrations of Cu. The peaks observed showed the Raman shift resulting in different peaks agreeing well with the boding and formation of barium titanate. The peaks of 269 cm^{-1} 443, and 519 cm^{-1} show the three E (TO) bonds that are in the presence of Titanium Oxygen bonds. The modes associated with Raman shift from 150 cm-1 to 350 cm-1 are related to the interaction of A-site (Ba site) and B-O (Ti-O) chains. The 319 cm-1 peak represents B1 which shows the tetragonal structure of $BaTiO_3$. The peaks from 450 cm-1 to 720cm-1 and around 700 represent the modes associated with the vibration of oxygen atoms in the BO_6 (TiO_6) octahedral. The spectrum of different concentrations with copper is disturbed due to the reason that at higher temperatures the stoichiometry of the $BaTiO_3$ is distorted as a result of overheating

4.4 FTIR:
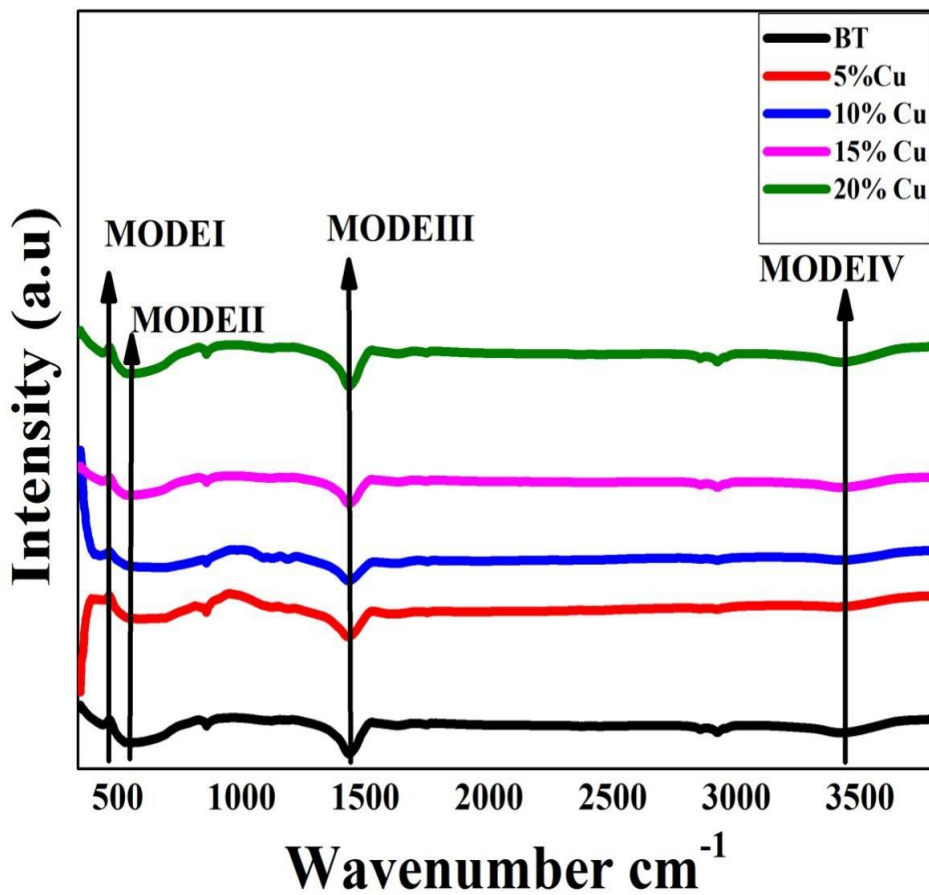
Figure 4-4 FTIR Spectroscopy

The band at 3410 cm^{-1} is related to O–H stretching modes of absorbed water by KBr pellets that were used for FT-IR spectroscopy. The peaks corresponding to Ba-carbonate are evident at 1630, 1427, 850, and 580cm^{-1}. The absorption band at 1427 cm^{-1} can is of C=O vibration due to small unavoidable traces of carbonate. Split in peak observed around 1000cm^{-1} after Cu addition suggests the distortion caused at Ti- O by the replacement of Ti by Cu.

4.5 Dielectric measurements

4.5.1 Dielectric constant vs temperature

The graph between temperatures vs. dielectric constant for barium titanate with 15% copper has shown some interesting results at a different rate of frequencies. As shown in the graph the dielectric constant is gradually increasing with temperature and frequencies but at a certain point after reaching there is a sharp drop seen in the graph showing the decrease in the dielectric constant. This sharp point is named as Curie point or Curie temperature T_C. The dielectric constant is strongly dependent on the temperature and frequency of the alternating current. After Curie temperature, the domains of materials do not remain stable and show some disorder in their trend. This phenomenon leads to toward sharp drop in a graph and shows decreasing trend of the dielectric constant.
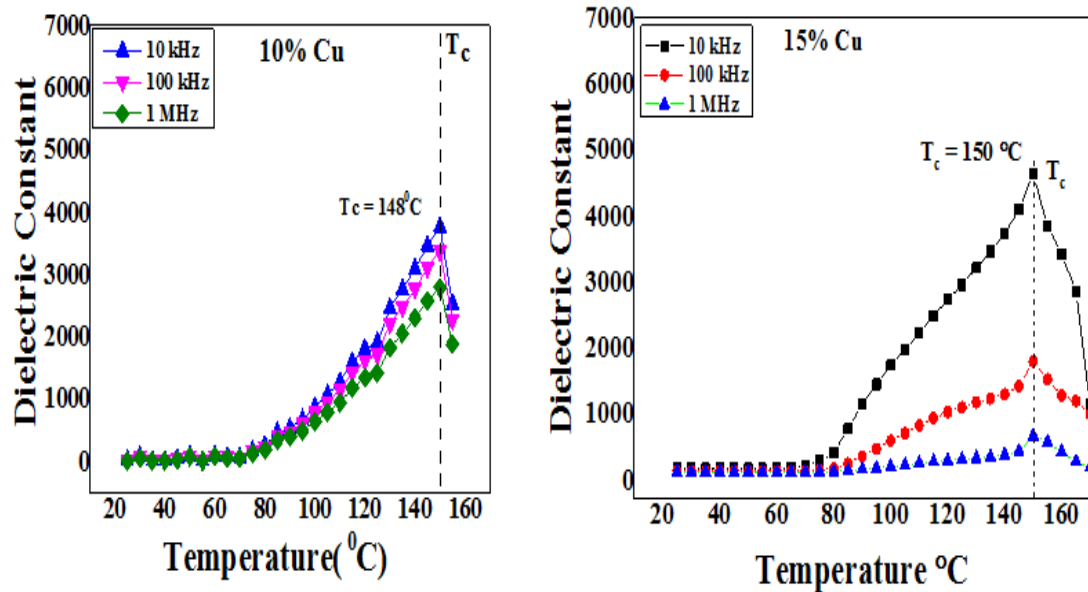

Fig 4-5 Dielectric constant vs. Temperature
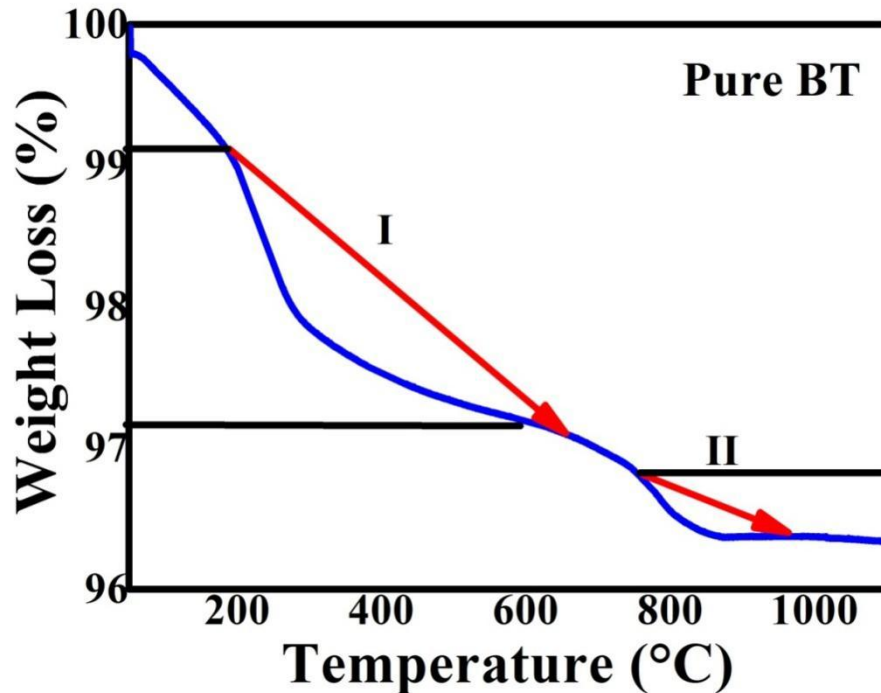
4.6   Temperature vs. weight loss:

Figure 4-6 Weight loss % vs. temperature

After all, there is a decreasing trend found in the barium titanate samples with an increasing amount of copper ranging (from 0 to 20%vol). The connection between barium titanate and copper is reduced due to the formation of cracks during the cooling process. The relative value and shrinkage have the same results while increasing from 0 to 20% of copper. Afterward, the decreasing behavior was observed due to the agglomeration of Ag nanoparticles approaching the percolation threshold as explained in the dielectric permittivity section. Thermo gravimetric analysis was performed to study the behavior of sinterability of synthesized composite materials. Several weight loss steps were revealed during the measurements of final results when the temperature is increased from zero to 1200 degrees. The overall weight loss is zero to 6% during increasing the temperature to 1200 degrees overall. During the test, the first weight loss is observed at 3000C. This is pointing toward the removal and burnout of residual organics arising during the synthesis of composites materials. Also the release of moisture during high temperatures. The second loss is observed in graph during the at 8000C because some amount of chemisorbed water or hydroxyl ion was incorporated in the BaTiO3-Cu samples. The first-order loss is higher than the second order

accordingly.

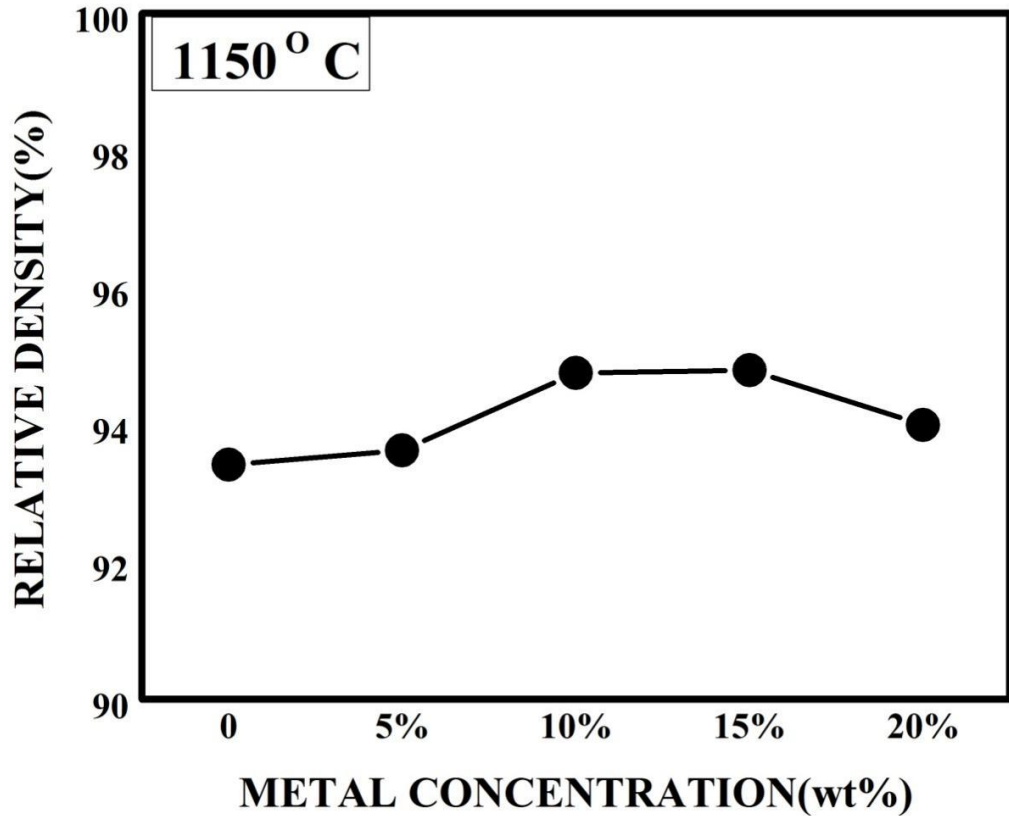## 4.7 Relative density vs. concentration

Figure 4-7 Relative density vs. Metal concentration

The density increased to a maximum value of ~95% at 15% and ~94% at 5% copper concentration as shown in Fig 4.8 Afterward, the increasing trend is observed with the increasing of silver content. The interconnection between BaTiO3 and Cu is reduced due to the formation of some macro cracks during cooling. A same decreasing trend was observed in shrinkage ratio as the Cu content was increased due to the rate of shrinkage difference between BaTiO3 and Cu. The relative density and shrinkage value have the same trend up to 5% copper content. Afterward, the increasing behavior was observed due to the agglomeration of Ag nanoparticles with approaching the percolation threshold as explained in the dielectric permittivity section.
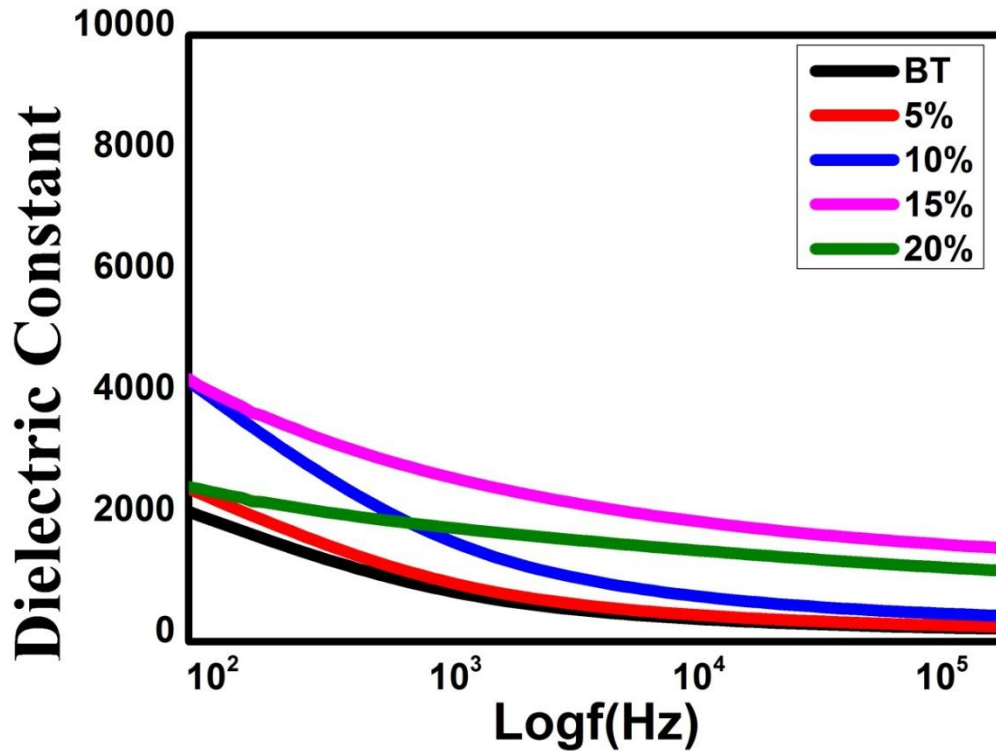
4.8 Dielectric vs. frequency

Figure 4-8 Dielectric constant vs. Frequency

The dielectric constant is showing a decreasing trend with an increase in the frequency ranging from the 100 Hz to Mega Hz .when we increase the frequency the domains inside the material do not respond. With the increasing frequency at the lower frequency the dielectric constant is higher but at the higher frequency it's gradually decreasing due to mismatch of relaxation time and frequency.

4.9 Real part vs. frequency

The real part of impedance with frequency is measured with the LCR meter. This showed the decreasing trend of the real part of impedance with the frequency. The increase in frequency and decrease in the real part of impedance inside the material relationship with the Maxwell Wagner model and the Koops model give decreasing trend.
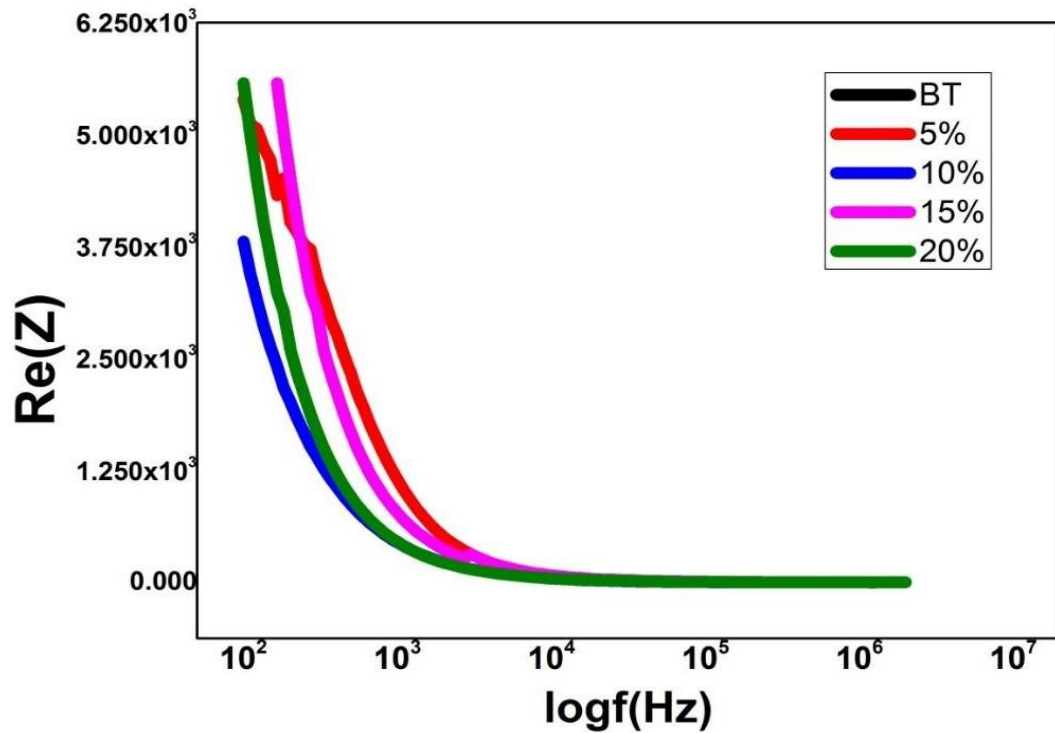
Figure 4-9 Real part vs Frequency

4.10 Imaginary part vs frequency

The imaginary part of the impedance simply showing reactance of the dielectric materials. The decreasing trend showing that the energy storage part of the material is decreasing with increasing frequency of the materials but this energy can be returned to the circuit by using some other modification or techniques. At the initial frequency range (200 Hz–1 MHz), the κ rapidly declines while at higher frequencies, the decrement rate allays and finally becomes constant. This behavior can be synchronized with the Maxwell Wagner Interfacial polarization model with Koop's phenomenological theory. Rendering to this model, the poorly conducting grain boundaries become more dynamic at the lower frequency owing to their internal morphological defects while highly conducting grains become competent at the high frequency. The obtained behavior at lower frequency is generally considered as a typical behavior of dielectric ceramics. At the lower frequency, the main contribution comes from different types of polarization, such as electronic, ionic, dipolar, and interfacial polarization.
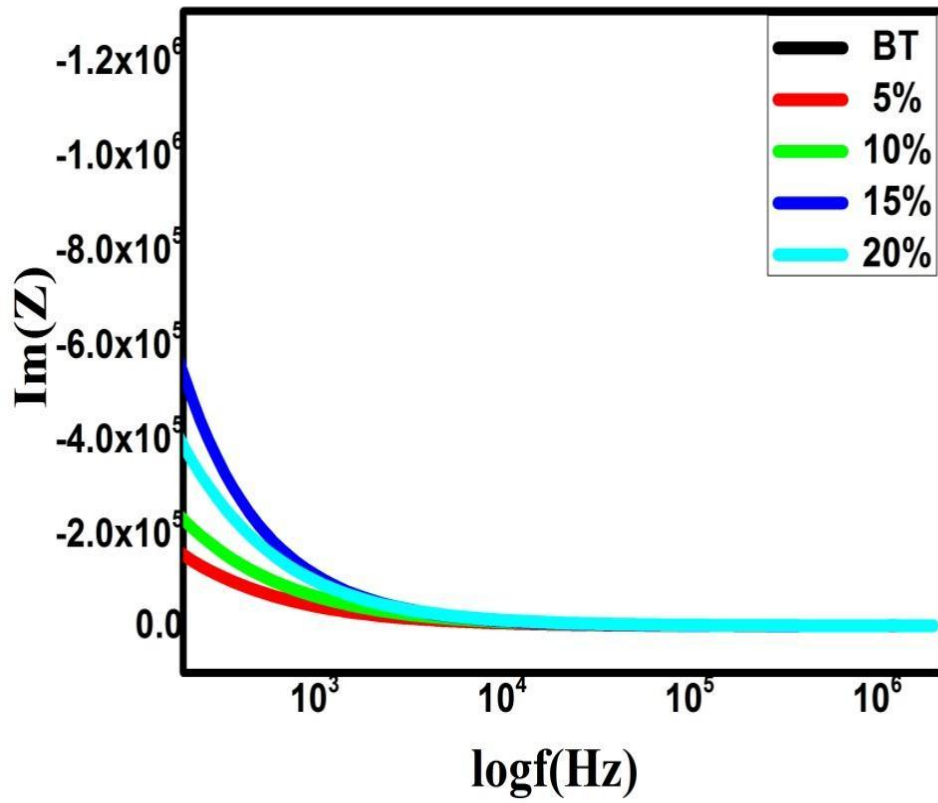
Figure 4-10 Imaginary part vs. Frequency

4.11 Tangent loss vs. frequency
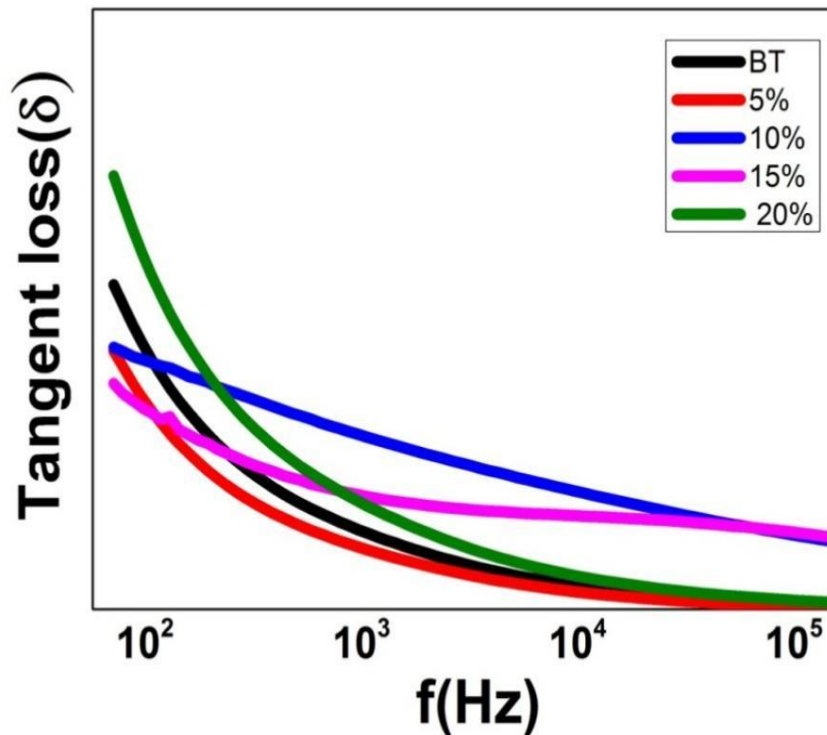
Figure 4-11 Tangent loss vs. frequency

The tangent loss of the 15% copper is showing the decreasing trend in the given graph. The frequency is independent of the geometry of the material. Tangent loss is the ratio between the real and imaginary parts of the impedance. The increase in frequency is giving more tangent loss as compared to a lower frequency. The losses occur due to the lattice imperfections. Stoichiometric defect, frenkel defects, schottky defects present in crystals.

4.12 Breakdown strength
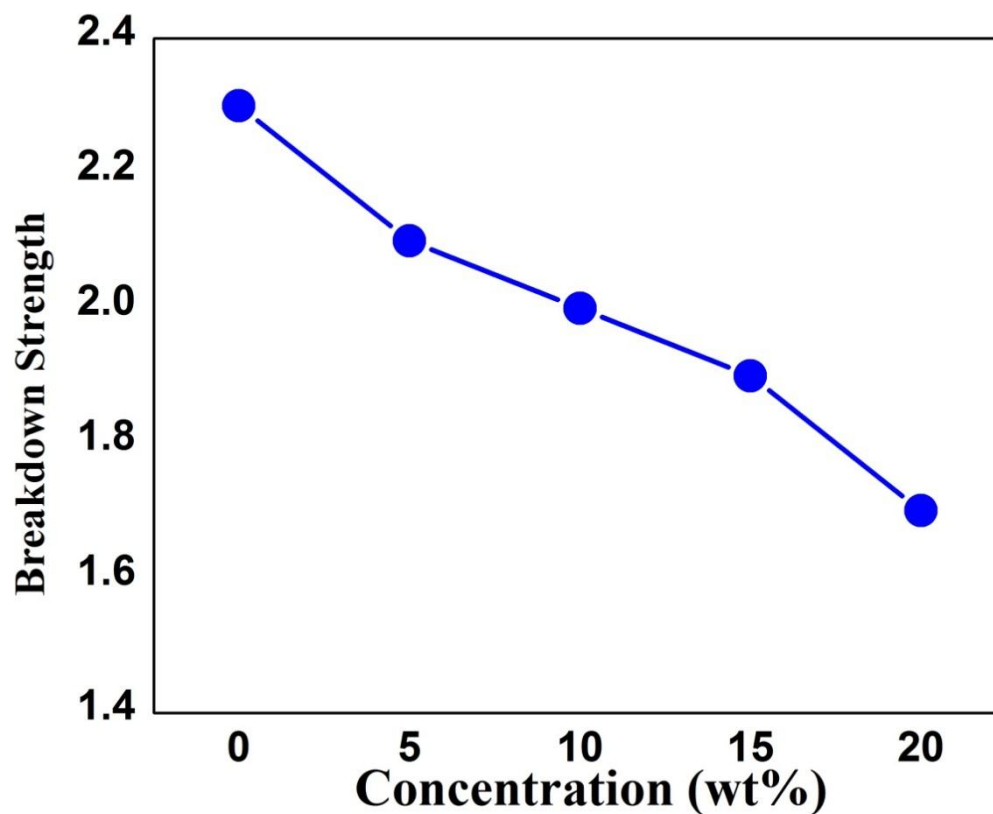
Figure 4-12   Breakdown strength vs. Concentration (wt%)

The influence of metal particles on the breakdown strength of barium titanate composite is shown in Fig.4.12. The breakdown strength is reduced with the increasing values of Cu particle. The low breakdown strength at a high concentration of Cu could be ascribed to the occurrence of agglomeration and a high value of conductivity. The decreasing values of breakdown strength occurred due to the shortening of the internal electrode gap, leading to the enhancement in the effective electric field . The breakdown strength is decreased by a third of the value of ~1.25 kV/mm at the Cu content of 15%

.

Conclusion

In the present work ceramic composites of barium titanate and copper were successfully synthesized. Different concentrations of copper were introduced into the barium titanate powder ranging from (5 to 20%). The XRD test confirmed the structure of barium titanate and composites. The increasing peak of copper showed the increasing concentration of copper. SEM images showed the uniform and homogenous crystallite size and showed no agglomeration of particles. No side reaction took place during the synthesis. Raman and FTIR spectroscopy was performed. Dielectric tests were performed for the dielectric properties. They showed the increasing trend of dielectric constant. Real and imaginary parts of dielectric pellets were found. The dielectric constant of 15% copper with barium titanate is found near 4500. The same result with increasing temperature was found at 10 KHz frequency at Curie temperature point. The dielectric loss is measured is 0.12. The behaviors of 15% Cu-BaTiO$_3$ are depicting the promising material for dielectric materials.

References

[1] Resonant X-ray Scattering |SheLaboratory" arpes.stanford.edu. Retrieved (2019)-07-10.

[2] Archived copy". Archived from the original on 2020-04-14. Retrieved 2013-03- 05.

[3] Agilent Technologies to Acquire Varian, Inc. for $1.5 Billion". Agilent. July 27, 2009.

[4] Brault, James W. (1996). "New Approach to high-precision Fourier transform spectrometer design". Applied Optics. 35 (16): 2891–

[5] 2896. Bibcode:1996ApOpt..35.2891B. doi:10.1364/AO.35.002891. PMID 21085438.

[6] Connes, J.; Connes, P. (1966). "Near-Infrared Planetary Spectra by Fourier Spectroscopy. I. Instruments and Results". Journal of the Optical Society of America. (7): 896–910. doi:10.1364/JOSA.56.000896.

[7] Stokes, Debbie J. (2008). Principles and Practice of Variable Pressure Environmental Scanning Electron Microscopy (VP-ESEM). Chichester: John Wiley & Sons. ISBN 978-0470758748.

[8] McMullan, D. (2006). "Scanning electron microscopy 1928– 1965". Scanning. 17 (3): 175–185. doi:10.1002/sca.4950170309. PMC 2496789.

[9] McMullan,D. (1988). "VonArdenne and the scanning electron microscope". Proc Roy Microsc Soc. 23: 283–288.

[10] Knoll, Max (1935)."Aufladepotentiel und Sekundäremission electron enbestrahlter Körper". Zeitschrift für Technische Physik. 16: 467–47.

[11] S. N. Mustafaeva, M. M. Asadov and K. S. Qahramanov, "Frequency-Dependent Dielectric Coefficients of TlInS2 Amorphous Films," Semiconductor Physics, Quantum Electronics & Optoelectronics, Vol. 10, No. 2, 2007, pp. 58-61.

[12] S. N. Mustafaeva, M. M. Asadov and V. A. Ramazanzade, "Dielectric Properties and Ac-conductivity of TlInS2 Single Crystals," Fizika Tverdogo Tela,

Vol. 38, No. 1, 1996,

[13] P. Smyth, "Dielectric Behaviour and Structure," McGrawHill, New York, 1965.

[14] A. J. Moulson and J. M. Herbert, "Electroceramics: Materials Properties Applications," Chapman & Hall, New York, 1990.

[15] GB 511204, von Ardenne, Manfred, "Improvements in electron microscopes", published 1939-08-15

[16] M. M. El-Desoky, "Dielectric Behaviour and AC Conductivity of Sodium Borate Glass Co ntaining CoO," Journal of Physics and Chemistry of Solids, Vol. 59, No. 9, 1998, pp. 1659-1666.

[17] A. B. Alles, R. Vanalstine, and W. Schulze, "Dielectric properties and aging of fast-fired barium titanate", Latin American Applied Research, 35 (2005) 29-

[18] . A. Beauger, J. C. Mutin, and J. C. Niepce, "Synthesis reaction of metatitanate BaTiO3: Part 1, effect of the gaseous atmosphere upon the thermal evolution of the system BaCO3-TiO2", Journal of Materials Science, 18 (1983) 3041-3046.

[19] A. Dixit, S. B. Majumder, A. Savvinov, R. S. Katiyar, R. Guo, and A. S. Bhalla, "Investigations on the sol-gel derived barium zirconium titanate thin films", Materials Letters, 56 (2002) 933-940.

[20] A. J. Dekker, "Solid State Physics", The Macmillan press LTD., 1958.

[21] A. W. Coats and J. Redfern, "Kinetic parameters from thermogravimetric data", Nature, 201 (1964) 68-69.

[22] A. Khawan and D. R. Flanagan, "Basics and applications of solid state kinetics: A pharmaceutical perspective", Journal of Pharmaceutical Sciences, 95 (2006) 472.

[24]. A. Lotnyk, S. Senz, and D. Hesse, "Formation of BaTiO3 thin film from (110) TiO2 rutile single crystals and BaCO3 by solid state reactions", Solid State Ionics, 177 (2006) 429.

[25]. B. D. Stojanovic, C. R. Foschini, M. A. Zaghete, and F. O. S. Veira, "Size effect on structure and dielectric properties of Nb-doped barium titanate", Journal of Materials Processing Technology, 143-144 (2003) 802-806.

[26]. B. D. Stojanovic, C. R. Foschini, V. B. Pavlovic, V. M. Pavlovic, V. Pejovic, and J. A. Varela, "Barium titanate screen-printed thick films", Ceramics International, 28 (2002) 293-298.

[27]. B. D. Stojanovic, C. R. Foschini, V. B. Pavlovic, V. M. Pavlovic, V. Pejovic, and J. A. Varela "Electrical properties of screen-printed BaTiO3 - 123 - thick films", Journal of the European Ceramics Society, 24 (2004) 1467- 1471.

[28]. B. Li, X. Wang, L. Li, H. zhou, X. Liu, X. Han,Y. Zhang, X. Qi, and X. Deng, "Dielectric properties of fine-grained BaTiO3 prepared by Sparkplasma-sintering", Materials Chemistry and Physics, 83 (2004) 23-28.

[29]. C. Doyle, "Estimating isothermal life from thermogravimetric data", J. Appl. Polym. Sci., 6 (1962) 639.

[30]. C. H. Lin, C. Y. Huang, and J. Y. Chang, "Increasing the conductivity of photorefractive BaTiO3 single crystals by doping Ru", Applied Surface Science, 208- 209 (2003) 340-344.

[31]. C. J. Xiao, C. Q. Jin, and X. H. Wang, "The fabrication of nanocrystalline BaTiO3 ceramics under high temperature and high pressure", Journal of materials Processing Technology, 209 (2009) 2033-2037.

[32]. C. Miclea, C. Tanasoiu, I. Stamulescu, C. F. Miclea, A. Gheorghiu, L. Amarande, M. Cioangher, and C. T. Miclea, "Microstructure and properties of barium titanate ceramics prepared by mechanochemical synthesis", Romanian Journal of Information Science and Technology, 10 [4] (2007) 335-345.

[33]. C. N. George, J. K. Thomas, H.P. Kumar, M. K. Suresh, V. R. Kumar, P. R. S.

Wariar, R. Jose, and J. Koshy, "Characterization, sintering and dielectric properties of nanocrystalline barium titanate synthesized through a modified combustion process", Materials Characterization, 60 (2009) 322-326. 17. C. Torres, M. S., C. A. Ribeiro, and H. E. Zorel, "BaTiO3 obtained through metallic stearate precursors", Materials Letters, 57 (2003) 1805- 1809.

[34]. C-S. His, Y-C. Chen, H. Jantunen, M-J. Wu, and T-C. Lin, "Barium titanate based dielectric sintered with a two-stage process", Journal of The European Ceramic Society, 28 (2008) 2581-2588. - 124 –

[35]. D. H. Yoon, J. Zhang, and B. I. Lee, "Dielectric constant and mixing model of BaTiO3 composite thick films", Materials Research Bulletin, 38 (2003) 765-772.

[36]. D. Prakash, B. P. Sharma, T. R. Rama Mohan, and P. Gopalan, "Flux additions in barium titanate: overview and prospects", Journal of Solid State Chemistry, 155 (2000) 86-95.

[37]. D. Segal, "Chemical synthesis of advanced ceramic materials", Cambridge University Press, (1991).

[38]. D. W. Richerson, "Modern ceramic engineering: Properties, processing, and use in design", Second Edition, Marcel Dekker, inc., (1992).

[39]. D. Zhang, D Zhou, S. Jiang, X. Wang, and S. Gong, "Effects of porosity on the electrical characteristics of current-limiting BaTiO3- based positive-temperature-coefficient (PTC) ceramic thermistors coated with elecroless nickel- phosphorous electrode", Sensors and Actuators, A112 (2004) 94-100.

[40]. E. Brzozowski and M. S. Castro, "Lowering the synthesis temperature of high-purity BaTiO3 powders by modifications in the processing conditions", Thermochimica Acta, 398 (2003) 123-129.

[41]. E. K. Reza, A. M. Hasan, and S. Ali, "Model fitting approach to kinetic analysis of non-isothermal oxidation of molybdenite", Iran. J. Chem. Eng.,

[42] [2] (2007) 119-123. 26. F-H. Lu, C-T. Wu, and C-y. Hung, "Barium titanate films synthesized by an anodic oxidation-based electrochemical method", Surface and Coatings Technology, 153 (2002) 276-283.

[43]. H. E. Kissinger, "Reaction kinetics in differential thermal analysis", Analytical Chemistry, 29 [11] (1957) 1702-1706.

[44]. H. Huang* and X. Yao, "Preparation of BaTiO3 thin films by mist plasma evaporation on MgO buffer layer", Ceramics International, 30 (2004) 1535-1538.

[45]. H. Huang**, X. Yao, M. Wang, and X. Wu, "BaTiO3 on LaNiO3 and Si thin films prepared by mist plasma evaporation", Journal of Crystal Growth, 263 (2004) 406-411

[46] H. Kakemoto, K-I. Kakimoto, A. Baba, S. Fujita, and Y. Masuda, "Ferroelectric properties of BaTi0.91(Hf0.5, Zr0.5)0.09O3 Thin films fabricated by pulsed laser deposition", Journal of the Ceramic Society of Japan, 109 [8] (2001) 651-655.

[47]. San Moon, Hyun-Wook Lee, Chang-Hak Choi, and Do Kyung Kim; "Influence of Ammonia on Properties of Nanocrystalline Barium Titanate Particles Prepared by a Hydrothermal Method", J. Am, Ceram. Soc., 1-6 (2012)

[48]   Xin Guo "Peculiar size effect in nanocrystalline BaTiO3", Acta Materialia, 61, 1748-1756 (2013)

[49]   P. Zheng, L. Zhang, Y. Q. Tan, C.L. Wang, "Grain-size effects on dielectric and piezoelectric properties of poled BaTiO3"Acta Materialia, 60, 5022-5030 (2012).

[50]. L. B. Kong, J. Ma, H. Huang, R. F.Zhang, and W. X. Que, "Barium titanate derived from mechanochemically activated powders", J. Alloy Compd.; 337, 226 (2002).

[51]   E. Brzozowski, M.S. Castro, "Lowering the Synthesis Temperature of High- Purity BaTiO3 Powders by Modifications in the Processing Conditions", Thermochimica Acta, 398, 1-2, 123- 131, (2003).

[52]   V. Berbenni, A. Marini, G. Bruni, " Effect of Mechanical Milling on Solid State Formation of BaTiO3 from BaTiO3- TiO2 (Rutile Mixtures", Thermochimica Acta,; 374, 151 (2001).

[53]. V. Pavlovic, B.D. Stojanovic, V.B. Pavlovic, Z. MarinkovicStanojevic, L. Zivkovic, and M.M. Ristic," Synthesis of BaTiO3 from a Mechanically Activated BaCO3-TiO2 System", Science of Sintering, 40 (2008) 21-26.

.

.